RESEARCH ARTICLE

AMERICAN JOURNAL OF
medical genetics
Neuropsychiatric Genetics

A Loss-of-Function Mutation in the *SLC9A6* Gene Causes X-Linked Mental Retardation Resembling Angelman Syndrome

Yumi Takahashi,[1] Kana Hosoki,[1] Masafumi Matsushita,[2] Makoto Funatsuka,[3] Kayoko Saito,[4] Hiroshi Kanazawa,[2] Yu-ichi Goto,[5] and Shinji Saitoh[1]*

[1]Department of Pediatrics, Hokkaido University Graduate School of Medicine, Sapporo, Japan

[2]Deparrtment of Biological Sciences, Graduate School of Science, Osaka University, Osaka, Japan

[3]Department of Pediatrics, Tokyo Womens' Medical University, Tokyo, Japan

[4]Institute of Medical Genetics, Tokyo Womens' Medical University, Tokyo, Japan

[5]Department of Mental Retardation and Birth Defect Research, National Institute of Neuroscience, National Center of Neurology and Psychiatry, Tokyo, Japan

Received 29 November 2010; Accepted 6 July 2011

SLC9A6 mutations have been reported in families in whom X-linked mental retardation (XMR) mimics Angelman syndrome (AS). However, the relative importance of *SLC9A6* mutations in patients with an AS-like phenotype or XMR has not been fully investigated. Here, the involvement of *SLC9A6* mutations in 22 males initially suspected to have AS but found on genetic testing not to have AS (AS-like cohort), and 104 male patients with XMR (XMR cohort), was investigated. A novel *SLC9A6* mutation (c.441delG, p.S147fs) was identified in one patient in the AS-like cohort, but no mutation was identified in XMR cohort, suggesting mutations in *SLC9A6* are not a major cause of the AS-like phenotype or XMR. The patient with the *SLC9A6* mutation showed the typical AS phenotype, further demonstrating the similarity between patients with AS and those with *SLC9A6* mutations. To clarify the effect of the *SLC9A6* mutation, we performed RT-PCR and Western blot analysis on lymphoblastoid cells from the patient. Expression of the mutated transcript was significantly reduced, but was restored by cycloheximide treatment, indicating the presence of nonsense mediated mRNA decay. Western blot analysis demonstrated absence of the normal NHE6 protein encoded for by *SLC9A6*. Taken together, these findings indicate a loss-of-function mutation in *SLC9A6* caused the phenotype in our patient.**

Key words: *SLC9A6*; sodium/hydrogen exchanger 6; Angelman syndrome; X-linked mental retardation; nonsense mediated mRNA decay

How to Cite this Article:
Takahashi Y, Hosoki K, Matsushita M, Funatsuka M, Saito K, Kanazawa H, Goto Y-I, Saitoh S. 2011. A Loss-of-Function Mutation in the *SLC9A6* Gene Causes X-Linked Mental Retardation Resembling Angelman Syndrome.
Am J Med Genet Part B 156:799–807.

INTRODUCTION

SLC9A6 mutations were first reported by Gilfillan et al. [2008] in families exhibiting an X-linked mental retardation (XMR) syndrome mimicking Angelman syndrome (AS). Angelman syndrome is characterized by severe developmental delay with absent or minimal speech, ataxia, easily provoked laughter, epilepsy, and microcephaly. The syndrome is caused by loss-of-function of the *UBE3A* gene which is subject to genomic imprinting. Patients with *SLC9A6* mutations resemble patients with AS, but also demonstrate distinctive clinical features including cerebellar atrophy, slow progression of symptoms, increased glutamate/glutamic acid peak on magnetic resonance spectroscopy (MRS), and lack of characteristic abnormalities seen AS patients examined using electroencephalography (EEG). Following the first report in 2008, in 2010 Schroer et al. reported two other families with AS due to *SLC9A6* mutations, and confirmed the findings of Gilfillan et al.

The *SLC9A6* gene is located on Xq26.3, and encodes the ubiquitously expressed Na^+/H^+ exchanger protein member 6, NHE6. The NHE protein family consists of nine members and includes

Grant sponsor: Ministry of Education, Culture, Sports, Science, and Technology, Japan; Grant number: 21591306.
*Correspondence to:
Shinji Saitoh, Department of Pediatrics, Hokkaido University Graduate School of Medicine, N-15, W-7, Kita-ku, Sapporo 060-8638, Japan.
E-mail: ss11@med.hokudai.ac.jp
Published online 2 August 2011 in Wiley Online Library (wileyonlinelibrary.com).
DOI 10.1002/ajmg.b.31221

NHE1-5 which is found in the plasma membrane, and NHE6-9 which is found in the membranes of intracellular organelles such as mitochondria and endosomes. NHE6 is predominantly present in the early recycling endosome membranes, and is believed to have a role in regulating luminal pH and monovalent cation concentration in intracellular organelles [Brett et al., 2002; Nakamura et al., 2005]. Moreover, Roxrud et al. demonstrated that NHE6 in combination with NHE9 participated in regulation of endosomal pH in HeLa cells by means of the procedure of co-depletion of NHE6 and NHE9 [Roxrud et al. 2009], indicating the significant role of NHE6 in fine-tuning of endosomal pH in human cells. In the brain, exocytosis from recycling endosomes is essential for the growth of dendritic spines which grow during long-term potentiation (LTP). In the absence of recycling endosomal transport, spines are rapidly lost, and LTP stimuli fail to elicit spine growth [Park et al., 2006]. Thus, NHE6 has an important role in the growth of dendritic spines, and also in the development of normal brain wiring. Thus far, five *SLC9A6* mutations have been reported in six AS families; two nonsense mutations, one inframe deletion, one frameshift deletion, and one splicing mutation [Gilfillan et al., 2008; Schroer et al., 2010]. The precise pathogenesis by which these mutations produce disease remains to be clarified.

The aim of this study was to clarify the incidence and importance of *SLC9A6* mutations in AS-like patients and patients with XMR, and to shed light on the molecular pathogenesis of disease due to *SLC9A6* mutations.

MATERIALS AND METHODS

Enrolled Patients

We examined 22 affected Japanese males clinically suspected of having AS but who lacked the genetic abnormalities reported in AS (AS-like cohort). These patients had AS excluded by having negative results for the *SNURF-SNRPN* DNA methylation test (which identifies a deletion, uniparental disomy, or imprinting defect) and *UBE3A* mutation screening (performed as described previously) [Saitoh et al., 2005]. We also examined DNA samples from 104 Japanese patients suspected of having XMR (XMR cohort). The XMR samples were collected as a part of a project for the Japanese Mental Retardation Consortium [Takano et al., 2008]. This study was approved by the Institutional Review Board of Hokkaido University Graduate School of Medicine, and written informed consent was obtained from the parents of the enrolled patients.

Mutation Analysis of the *SLC9A6* Gene

We amplified each exon, including exon–intron boundaries, of the *SLC9A6* gene using polymerase chain reaction (PCR), and all amplicons were directly sequenced on an ABI 3130 DNA analyzer (Applied Biosystems, Foster City, CA) using BigDye Terminator V.1.1 Cycle Sequencing Kit (Applied Biosystems). *SLC9A6* encodes two alternatively spliced transcripts produced from alternative splicing donor sites in exon 2 which give rise to a long form designated as variant 1, and a short form called variant 2. Variant 1 and variant 2 code for NHE6.1 (isoform a) and NHE6.0 (isoform b), respectively (Fig. 1). The primers were designed to amplify each transcript variant. The primers sequence used for amplification and sequencing are available on request. Genomic DNA (10 ng) extracted from peripheral blood was amplified in a total PCR volume of 20 μl containing 1× buffer, 0.4 μM of each primer (forward/reverse), 0.18 mM dNTPs, 0.5 U AmpliTaq Gold® DNA Polymerase (Applied Biosystems). The PCRs for all exons except exon one were performed at 94°C for 10 min followed by 30 cycles of 94°C for 30 sec, 55°C for 30 sec, 72°C for 30 sec, then one cycle at 72°C for 7 min. The high CpG content of exon 1 required it to be amplified in a total reaction volume of 20 μl containing 1× buffer, 0.4 μM of each primer, 0.2 mM dNTPs, 0.4 U Phusion® Hot Start High-Fidelity DNA Polymerase (Finnzymes, Vantaa, Finland), and 3% DMSO. The thermocycling conditions for exon 1 were 98°C for 3 min followed by 35 cycles of 98°C for 10 sec, 65°C for 30 sec and 72°C for 30 sec and then one cycle of 72°C for 5 min. The PCR products were purified with Wizard® PCR Preps DNA Purification System (Promega, Madison, WI) prior to sequencing. All mutations are referred to in relation to reference sequence NM_001042537.

Cell Culture and Cycloheximide Treatment

Epstein–Barr virus (EBV)-transformed lymphoblastoid cells lines were established from peripheral blood cells using standard methods. To prevent potential degradation of transcripts containing premature translation termination codons (PTCs) by nonsense mediated mRNA decay (NMD), lymphoblastoid cells from the patient with the *SLC9A6* mutation and normal controls were treated with 100 μg/ml cycloheximide (CHX) (Sigma, St. Louis, MO). This compound interferes with NMD through inhibition of protein synthesis [Aznarez et al., 2007]. CHX or a 0.1% DMSO control vehicle was used 4 hr prior to RNA extraction from the cell lines [Carter et al., 1995].

RT-PCR

Total RNA from cultured lymphoblastoid cells from the patient and four normal controls, was extracted using the RNAqueous® Kit (Applied Biosystems). Reverse transcription was performed using 100 ng of total RNA and the High-Capacity cDNA Reverse Transcription Kit (Applied Biosystems) in a total reaction volume of 20 μl containing 1× Random primers, 4 mM dNTP mix, 2.5 U of Multiscribe™ Reverse Transcriptase, and 1 μl of RNase Inhibitor. The reactions were incubated at 25°C for 10 min, then at 37°C for 120 min and then followed by 85°C for 5 min to inactivate the reverse transcriptase. Complementary DNA was then amplified using a primer set designed to amplify exon 2–5; forward 5′-GTCTTTTGGTGGGCCTTGT-3′, reverse 5′-GTCCCGTTACC-TTCATCAG-3′. PCR products for NHE6.1 (transcript variant 1) and NHE6.0 (transcript variant 2) were 399 and 303 bp, respectively.

Real-Time Quantification of *SLC9A6* mRNA

To measure *SLC9A6* transcript variant 1 and variant 2, both of which are alternative splicing products, primers and TaqMan® MGB probes were designed with Primer® Express Software (Applied Biosystems; Fig. 1). The Primer and MGB probe sequence

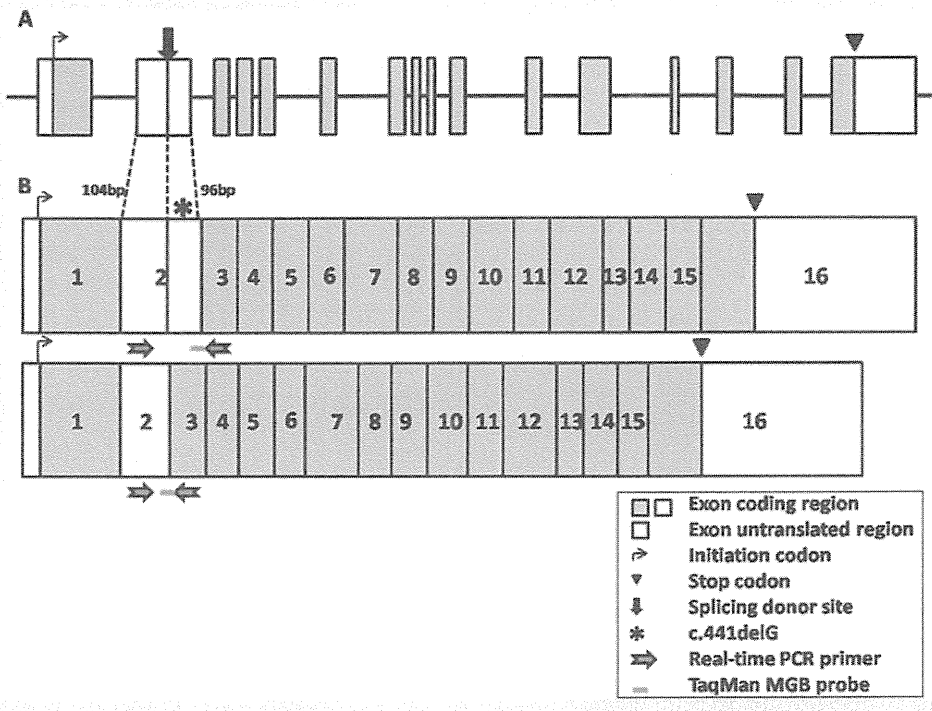

FIG. 1. A: Genomic structure of the *SLC9A6* gene. B: Two alternatively spliced transcripts of the *SLC9A6* gene. Above: *SLC9A6* transcript variant 1 (encodes NHE6.1 or isoform a). Below: *SLC9A6* transcript variant 2 (encodes NHE6.0 or isoform b). The location of the *SLC9A6* mutation in our patient is shown with *. Primers and probes used in real-time quantitative PCR are shown (horizontal arrows).

for variant 1 were forward primer 5′-TGAGTATATGCTGAAAGGAGAGATTAGTTC-3′, reverse primer 5′-GATAGGAGGAAGTAATATGTTGAAAAATACTTC-3′, TaqMan MGB probe 5′-CTTAGAAAGGTTACTTTTGATCC-3′; and for variant 2 forward primer 5′-CTGTGAAGTGCAGTCAAGTCCAA-3′, reverse primer 5′-GATAGGAGGAAGTAATATGTTGAAAAATACTT-3′, TaqMan MGB probe 5′-CTACCTTACTGGTTACTTTTGA-3′. Human *GAPDH* MGB probe and primers purchased from Applied Biosystems were used as the internal control. Patient cDNA was transcribed from 10 ng of total RNA in a total volume of 25 µl containing 1× TaqMan® Universal PCR Master Mix (Applied Biosystems), 0.9 µM of each primer (sense/antisense) and 0.25 µM of probe. Thermocycling was 95°C for 10 min, followed by 40 cycles of 95°C for 15 sec and 60°C for 1 min. Real-time quantitative PCR was performed using the ABI PRISM 7700 (Applied Biosystems). The $2^{-\Delta\Delta Ct}$ method was used for relative quantification.

Western Blot Analysis

HeLa cells and cultured lymphoblastoid cells from the patient, mother and normal controls were washed with phosphate buffered saline and suspended in lysis buffer (phosphate buffered saline containing 1% Triton-X, 1 µg/ml aprotinin, 1 µg/ml pepstatin A, and 1 µg/ml leupeptin). HeLa cells expressing the NHE6.1 were used as a control. The cells were disrupted by sonication and centrifuged at 20,000*g* for 10 min at 4°C. The supernatants were then resolved by SDS-polyacrylamide electrophoresis and transferred to polyvinylidene fluoride membrane (Millipore, Billerica, MA). NHE6 was detected with rabbit polyclonal anti-NHE6 antibody [Ohgaki et al., 2008], anti-rabbit IgG antibody conjugated with horseradish peroxidase (Vector Laboratories, Burlingame, CA) and chemiluminescence reagent (ECL Western Blotting Detection System; GE Healthcare, Waukesha, WI).

RESULTS

Identification of a *SLC9A6* Mutation

We identified only one male patient with a frameshift mutation (c.441delG, p.S147fs) in exon 2, out of 22 male patients in the AS-like cohort (Fig. 2). This frameshift mutation causes a PTC. His healthy mother was heterozygous for the mutation.

No mutation in the *SLC9A6* gene was identified in the XMR cohort. However, two common polymorphisms (rs2291639, rs2307131), and one putative novel polymorphism in intron 12 (c.1692 +10 A>G) were detected.

Clinical Features of the Patient With the *SLC9A6* Mutation

The affected male patient at birth suffered from mild neonatal asphyxia, however he had no other perinatal problems. His parents

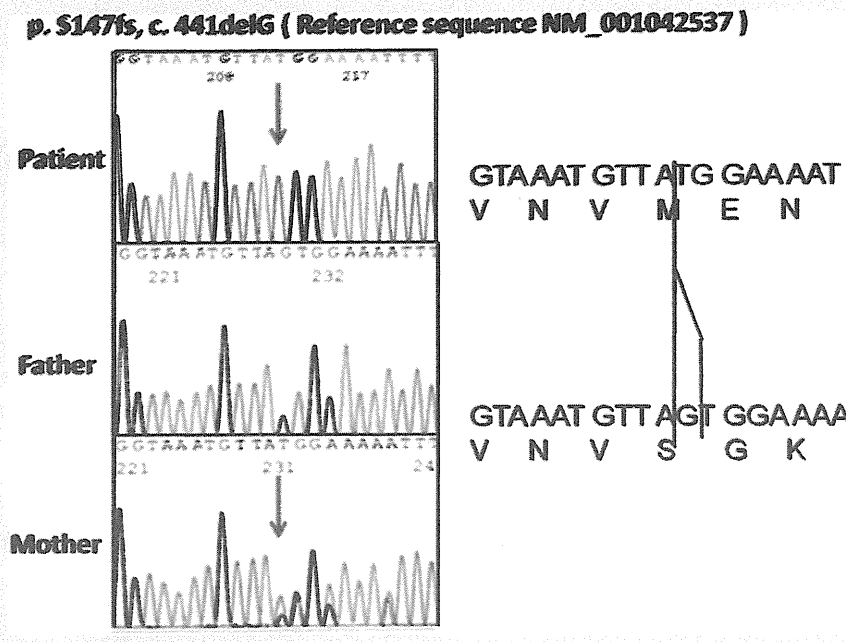

FIG. 2. Chromatographs showing the *SLC9A6* mutation in our patient, and the equivalent genomic region in both his parents. The mutation c.441delG is located in exon 2 and is only present in transcript variant 1. His mother was heterozygous for this mutation, while his father did not have the mutation. This mutant transcript leads to premature protein truncation. The mutation is described relative to reference sequence NM_001042537. [Color figure can be seen in the online version of this article, available at http://onlinelibrary.wiley.com/journal/10.1002/(ISSN)1552-485X]

were non-consanguineous and he did not have any family history of neurological diseases. Although formal clinical assessment was not conducted to the mother, she is healthy and does not have intellectual disability. His clinical features are summarized in Table I. He showed typical findings of AS; severe developmental delay with absence of verbal language, generalized hypotonia, easily provoked laughter, epilepsy, ataxia, strabismus, and microcephaly. His occipitofrontal head circumference at birth was 33.8 cm (+0.4 SD), but his head growth has decelerated into 51.5 cm (−3.0 SD) at 18 years of age. He acquired head control at three months of age, sat and crawled at 6 months of age, and walked unassisted at 18 months of age. His first epileptic attack occurred at 4 years of age. After this first attack, he lost his ability to walk until he was 5 years old. His epileptic attacks consisted of multiple types of seizures, and they were difficult to control with ACTH or several anti-epileptic drugs. TRH treatment improved his awakening and activity levels, and he transiently acquired the ability to walk. However, subsequently his ability to walk was lost, probably due to exacerbation of ataxia. His deep tendon reflex was not increased and no other features of spasticity or peripheral neuropathy were identified. His EEG findings included a background frequency of 5–6 Hz theta waves and spontaneous appearance of 3 Hz diffuse high voltage slow waves. TRH did not change the frequency of his seizures or his EEG findings. He showed no cerebellar atrophy on magnetic resonance imaging (MRI) at 5 years of age. MRS was not performed. He had a normal G-banding karyotype.

Downregulation of the *SLC9A6* Variant 1 in the Patient With the Mutation

The identified mutation c.441delG is located in exon 2 and is only present in variant 1 (Fig. 1). Therefore, the mutation only affects NHE6.1, leaving NHE6.0 intact. Reverse transcriptase PCR demonstrated that *SLC9A6* variant 1 mRNA expression decreased in our patient (Fig. 3A) compared to that in four normal controls. On the other hand, variant 2 expression was increased in the patient compared to the controls. To further investigate mutant *SLC9A6* gene expression, real-time quantitative PCR (qPCR) was performed using cDNA from the patient and normal controls. Quantitative PCR confirmed that *SLC9A6* variant 1 was significantly downregulated in the patient, while it was not downregulated in normal controls (Fig. 4A). Furthermore, the *SLC9A6* variant 2 mRNA in the patient was significantly increased compared to normal controls (Fig. 4B).

Nonsense Mediated Decay Was Involved in the Downregulation of Mutant *SLC9A6* in the Patient

To investigate the possible involvement of NMD in the downregulation of mutant *SLC9A6* in the patient's lymphoblastoid cells, we treated the cells with CHX. After CHX treatment, the expression level of *SLC9A6* variant 1 increased compared to normal control samples on RT-PCR (Fig. 3B). It was also proved that the expression level of variant 1 was significantly increased by performing qPCR, while the expression level in normal control samples

TABLE I. Clinical Findings in Affected Males Previously Reported and Our Patient

Family number: report affected males number (examined number)	1: Gilfillan et al. [2008] 3 (3)	2: Gilfillan et al. [2008] 2 (1)	3: Gilfillan et al. [2008] 3 (3)	4: Gilfillan et al. [2008], Christianson et al. [1999] 16 (4)	5: Schroer et al. [2010] 6 (6)	6: Schroer et al. [2010] 1 (1)	Our patient
Development and behavior							
Profound delay	+	+	+	+	+	+	+
Verbal language absent	+	+	+	+	+	+	+
Easily provoked laughter	+	+	+	+	3/6	−	+
CNS findings							
Epilepsy	+	+	+	+	+	+	+
Ataxia	+	+	+	+	NR	NR	+
Hyperkinetic movements	2/3	−	+	−	2/6	NR	−
Strabismus	+	+	+	+	5/6	+	+
Physical findings							
Microcephaly	+	+	+	3/4	5/6	+	+
Open mouth + drooling	2/3	+	+	NR	4/6	+	+
Swallowing difficulty	2/3	+	1/3	1/4	NR	+	−
Flexed arms	+	NR	1/3	+	3/6	−	−
Electroencephalography							
Epileptiform activity	+	+	+	+	+	+	+
Background activity	10–11 Hz	1.5–3 Hz	4–7 Hz	3–6 Hz to 11–14 Hz	NR	α rhythm	5–6 Hz
Brain MRI/autopsy							
Cerebellar atrophy	1/3	NR	NR	2/4	2/6	+	−
Mutation	p.E287_S288del c.936_941delAAAGTG	p.R500X c.1574C → T	p.V176_201del c.679 +1 delGTAA	p.H203fs c.684_685delAT	p.R500X c.1574C → T	p.Q437X c.1391C → T	p.S147fs c.441delG

+, present with all the patients; −, not present; NR, not recorded.

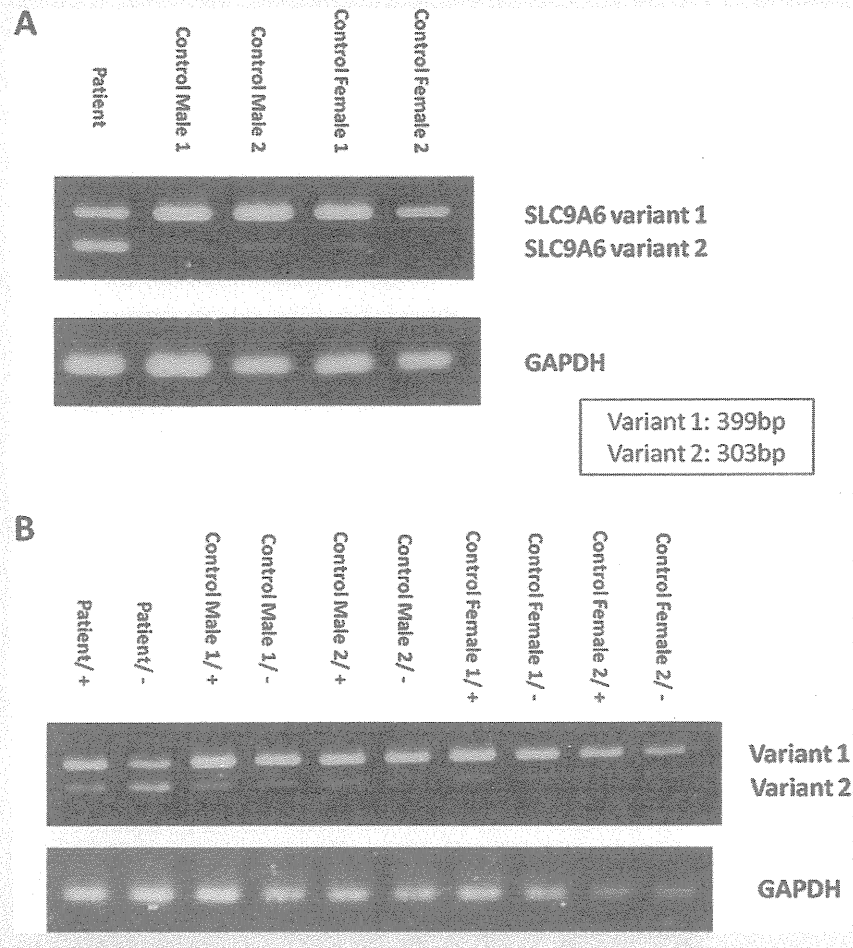

FIG. 3. RT-PCR amplification of the *SLC9A6* gene. A: *SLC9A6* variant 1 mRNA expression was decreased in the patient compared to that in four normal controls. On the other hand, variant 2 expression was increased in the patient compared to that in the controls. B: CHX treatment increases the mutant *SLC9A6* variant 1 mRNA expression, leading to similar expression levels in the patient and four normal controls samples. (+) After CHX treatment, (−) no CHX treatment.

was unchanged (Fig. 4A). The expression level of *SLC9A6* variant 2 increased in all samples after CHX treatment, however the increase was significant only in control samples (Fig. 4B).

Decreased Expression of the NHE6 Protein From Mutant *SLC9A6*

Western blotting was performed to investigate expression of the NHE6 protein in the homogenate of lymphoblastoid cell lines from the patient and his mother. As a result, protein expression of NHE6.1 was not detected in the patient (Fig. 5A,B). The same NHE6.1 was detected in HeLa cells and cells from the patient's mother as well as in the controls. NHE6.0, which was expected to be 10–20 kDa smaller than NHE6.1on SDS–PAGE [Ohgaki et al., 2008], was not detected in any sample (Fig. 5B).

DISCUSSION

In this study we investigated 22 male AS-like patients and 104 male patients with XMR, and identified only one AS-like patient with a *SLC9A6* frameshift mutation. This result further confirms *SLC9A6* is not a major cause of AS-like cases, as reported by Fichou et al. [2009]. Although the number of patients with XMR in this study was small, *SLC9A6* is likely to account for only small proportion of XMR cases.

Patients with *SLC9A6* mutations reported by Gilfillan et al., exhibit cardinal features similar to those of AS including severe developmental delay, mental retardation with absent or minimal use of words, easily provoked laughter, ataxia, epilepsy, hyperkinetic movement, nystagmus, and microcephaly.

Gilfillan et al. also identified possible features of difference between these patients and AS patients, including slow progression of symptoms, thin body, cerebellar atrophy, increased glutamate/

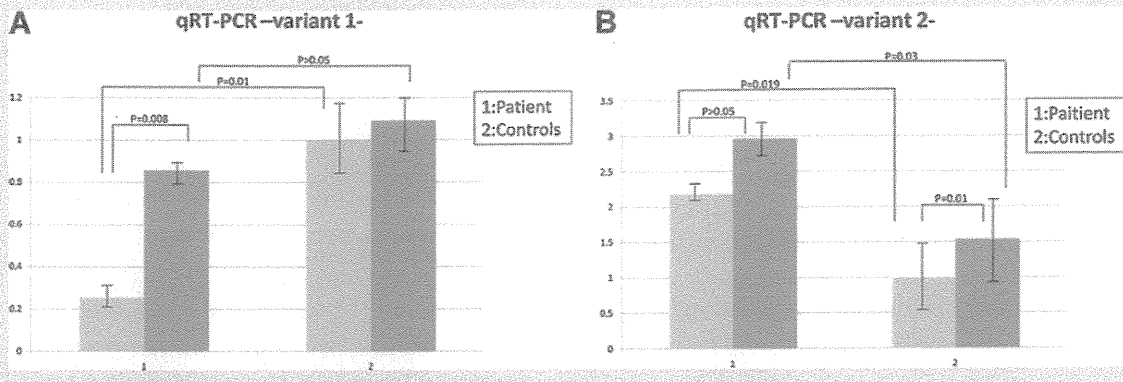

FIG. 4. Real-time quantitative PCR in samples from cell lines from the patient and four normal controls containing two males and two females. The light gray bars indicate the expression levels of *SLC9A6* before CHX treatment, while deep gray bars after CHX treatment. We performed statistical analysis using paired and unpaired Student's *t*-test. Error bars show standard deviation. A: The *SLC9A6* variant 1 was significantly downregulated in samples from the patient while it was not downregulated in samples from four normal controls. After CHX treatment, expression level of the *SLC9A6* variant 1 mRNA in the patient's sample was significantly increased. B: The *SLC9A6* variant 2 in the patient's sample was significantly increased compared to normal controls. Expression level of *SLC9A6* variant 2 increased in all samples after CHX treatment, but a significant increase was only seen in samples from controls.

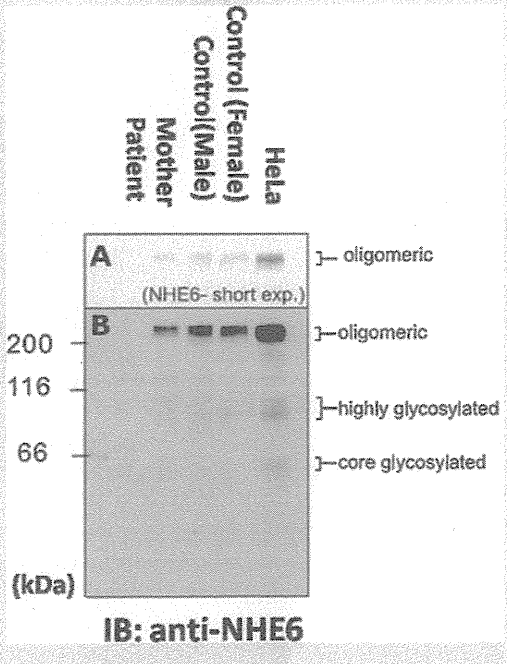

FIG. 5. Protein expression of NHE6 in cultured lymphoblastoid cells and HeLa cells. In the patient, no protein expression of NHE6 isoforms was detected with Western blotting using anti-NHE6 antibody. A: A cropped image taken using a short exposure time demonstrating the oligomeric form of NHE6. Protein size in kDa is shown by numbers on the left of the image. B: A chemiluminescence image of Western blotting taken with a longer exposure time.

glutamic acid peak on MRS, and rapid frequency of 10–14 Hz waves on EEG (Table I). Our patient lost his ability to walk although he did not demonstrate spasticity, demonstrating a slowly progressive clinical course consistent with findings in Gilfillan's report. Indeed, slow progression may be a distinctive clinical feature for patients with *SLC9A6* mutations. One of the families which Gilfillan et al. investigated was previously reported by Christianson et al. [1999], and designated as Christianson syndrome. Schroer et al. reported patients with Christianson syndrome, and they showed that the patients demonstrated an AS-like phenotype. However, while the clinical features of our patient were consistent with those of most patients previously reported by Gilfillan, there were differences including the EEG findings and lack of cerebellar atrophy. Despite this, our patient did meet the diagnostic criteria for AS [Williams et al., 2006]. Therefore, this study further demonstrated that a patient with a *SLC9A6* mutation may resemble patients with AS. Further, this striking similarity between patients with AS and those with *SLC9A6* mutations suggests a possible relationship between the gene function of *UBE3A* and *SLC9A6* in the developing brain.

Our patient's mutation created a frameshift resulting in 7 missense amino acids followed by a stop codon. This mutation was present only in *SLC9A6* transcript variant 1. *SLC9A6* mRNA has two transcript variants caused by alternative splicing in exon 2 (Fig. 1), but the role of each variant has not been clarified. The mutation detected in our patient only affects variant 1 sequence, but the phenotype of the patient was as severe as those in previously reported patients. Therefore, our finding suggests that the NHE6.1 plays an important role in brain function.

Nonsense mediated decay is involved in regulating the expression of alternatively spliced forms containing PTCs [Lareau et al., 2007; Ni et al., 2007]. Since the identified mutation was predicted to result in a PTC, we speculated that NMD could be involved in disease pathogenesis. The result of qRT-PCR showed a significant

decrease in *SLC9A6* variant 1 mRNA expression in the patient sample. This reduction was restored by CHX treatment, while *SLC9A6* variant 1 expression was unaltered by CHX treatment in normal control samples. Expression of *SLC9A6* variant 2 in the patient on the other hand, was significantly increased compared to that in control samples, however it was not influenced by CHX treatment. Therefore, the c.441delG mutation in the patient seems to have modified the alternative splicing pattern, leading to an increase in variant 2 expression. Alternatively, low variant 1 could trigger a regulatory feed back on transcription causing the apparent increase in variant 2 expression. A mutation causing premature protein truncation could alter the splicing pattern and lead to exon skipping, use of alternative splice sites, and intron retention [Hentze and Kulozik, 1999; Mendell and Dietz, 2001]. Our results indicated that the c.441delG mutation caused a PTC altered the splicing pattern, and activated NMD machinery then downregulated *SLC9A6* variant 1 expression.

As protein NHE6.1 was not detected, this indicates an absence of intact NHE6.1. NHE6.0 was also not detected. These findings conclusively indicated that the identified mutation should cause total loss-of-function. Recently, Garbern et al. identified cases with an in-frame deletion of three amino acids, who showed milder dysmorphic features and higher gross motor abilities than those in cases previously reported [Garbern et al., 2010]. Their in-frame deletion should not cause total loss-of-function but create a mildly dysfunctional protein. Therefore, severe phenotypes including severe developmental delay and progressive neurological deterioration may be caused by truncated mutations and less severe phenotypes may be caused by missense or in-frame mutations, and such mild phenotypes are likely missed in patients with mild developmental delay.

Given that the *SLC9A6* variant 2 was upregulated, we speculated that upregulated variant 2 might partially compensate for the absence of NHE6.1. However, we could not establish the upregulation of the NHE6.0 protein, rather it was not detected in the patient's lymphoblastoid cells. NHE6.0 may be unstable compared to NHE6.1. Alternately, NHE6.0 translation may be inhibited. Further investigation is required to definitively answer this question.

NHE6 is found in the membranes of early recycling endosomes and transiently in plasma membranes. Its distribution is regulated by RACK1 [Ohgaki et al., 2008]. Recycling endosomal trafficking is essential for the growth of dendritic spines during LTP in the brain [Park et al., 2006]. The function of the protein product of *UBE3A*, E3 ubiquitin ligase, is also associated with dendritic spine morphology. Mice with a maternal null mutation in *Ube3a* are also reported to have defects in LTP, and manifest motor and behavioral abnormalities [Jiang et al., 1998]. In a recent study, *Ube3a* deficient mice demonstrated dendritic spine dysmorphology [Dindot et al., 2008]. Thus, *UBE3A* and *SLC9A6* could interact in a common pathway involved in dendritic spine development, with a mutation in either leading to an AS-like phenotype.

ACKNOWLEDGMENTS

The authors thank Dr. Tadashi Ariga for critical reading of the manuscript.

REFERENCES

Aznarez I, Zielenski J, Rommens JM, Blencowe BJ, Tsui LC. 2007. Exon skipping through the creation of a putative exonic splicing silencer as a consequence of the cystic fibrosis mutation R533X. J Med Genet 44: 341–346.

Brett CL, Wei Y, Donowitz M, Rao R. 2002. Human Na(+)/H(+) exchanger isoform 6 is found in recycling endosomes of cells, not in mitochondria. Am J Cell Physiol 5:1031–1041.

Carter MS, Doskow J, Morris P, Li S, Nhim RP, Sandstedt S, Wilkinson MF. 1995. A regulatory mechanism that detects premature nonsense codons in T-cell receptor transcripts in vivo is reversed by protein synthesis inhibitors in vitro. J Biol Chem 270:28995–29003.

Christianson AL, Stevenson RE, van der Meyden CH, Pelser J, Theron FW, van Rensburg PL, Chandler M, Schwartz CE. 1999. X linked severe mental retardation, craniofacial dysmorphology, epilepsy, ophthalmoplegia, and cerebellar atrophy in a large South African kindred in localized to Xq24–q27. J Med Genet 36:759–766.

Dindot SV, Antalffy BA, Bhattacharjee MB, Beaudet AL. 2008. The Angelman syndrome ubiquitin ligase localizes to the synapse and nucleus, and maternal deficiency results in abnormal dendritic spine morphology. Hum Mol Genet 17:111–118.

Fichou Y, Bahi-Buisson N, Nectoux J, Chelly J, Heron D, Cuisset L, Bienvenu T. 2009. Mutation in the *SLC9A6* gene is not a frequent cause of sporadic Angelman-like syndrome. Eur J Hum Genet 17:1378–1380.

Garbern JY, Neumann M, Trojanowski JQ, Lee VM, Feldman G, Norris JW, Friez MJ, Schwartz CE, Stevenson R, Sima AA. 2010. A mutation affecting the sodium/proton exchanger, *SLC9A6*, causes mental retardation with tau deposition. Brain 133:1391–1402.

Gilfillan GD, Selmer KK, Roxrud I, Smith R, Kyllerman M, Eiklid K, Kroken M, Mattingsdal M, Egeland T, Stenmark H, Sjoholm H, Server A, Samuelsson L, Christianson A, Tarpey P, Whibley A, Stratton MR, Futreal A, Teague J, Edkins S, Gecz J, Turner G, Raymond FL, Schwartz C, Stevenson RE, Undlien DE, Stromme P. 2008. *SLC9A6* mutations cause X-linked mental retardation, microcephaly, epilepsy, and ataxia, a phenotype mimicking Angelman Syndrome. Am J Hum Genet 82: 1003–1010.

Hentze MW, Kulozik AE. 1999. A perfect message: RNA surveillance and nonsense-mediated decay. Cell 96:307–310.

Jiang YH, Armstrong D, Albrecht U, Atkins CM, Noebels JI, Eichele G, Sweatt JD, Beaudet AL. 1998. Mutation of the Angelman ubiquitin ligase in mice causes increased cytoplasmic p53 and deficits of contextual learning and long-term potentiation. Neuron 21:799–811.

Lareau LF, Inada M, Green RE, Wengrod JC, Brenner SE. 2007. Unproductive splicing of SR genes associated with highly conserved and ultraconserved DNA elements. Nature 446:926–929.

Mendell JT, Dietz HC. 2001. When the message goes awry: Disease-producing mutations that influence mRNA content and performance. Cell 107:411–414.

Nakamura N, Tanaka S, Teko Y, Mitsui K, Kanazawa H. 2005. Four Na^+/H^+ exchanger isoforms are distributed to Golgi and post-Golgi compartments and are involved in organelle pH regulation. J Biol Chem 280:1561–1572.

Ni JZ, Grate L, Donohue JP, Preston C, Nobida N, O'Brien G, Shiue L, Clark TA, Blume JE, Ares M, Jr. 2007. Ultraconserved elements are associated with homeostatic control of splicing regulators by alternative splicing and nonsense-mediated decay. Genes Dev 21:708–718.

Ohgaki R, Fukura N, Matsushita M, Mitsui K, Kanazawa H. 2008. Cell surface levels of organellar Na^+/H^+ exchanger isoform 6 are regulated by interaction with RACK1. J Biol Chem 283:4417–4429.

Park M, Salgado JM, Ostroff L, Helton TD, Robinson CG, Harris KM, Ehlers MD. 2006. Plasticity-induced growth of dendritic spines by exocytic trafficking from recycling endosomes. Neuron 52:817–830.

Roxrud I, Raiborga C, Gilfillan GD, Strømmed P, Stenmark H. 2009. Dual degradation mechanisms ensure disposal of NHE6 mutant protein associated with neurological disease. Exp Cell Res 135:3014–3027.

Saitoh S, Wada T, Okajima M, Takano K, Sudo A, Niikawa N. 2005. Uniparental disomy and imprinting defects in Japanese patients with Angelman syndrome. Brain Dev 27:389–391.

Schroer RJ, Holden KR, Tarpey PS, Matheus MG, Griesemer DA, Friez MJ, Fan JZ, Simensen RJ, Stromme P, Stevenson RE, Stratton MR, Schwartz CE. 2010. Natural history of Christianson syndrome. Am J Med Genet Part A 152A:2775–2783.

Takano K, Nakagawa E, Inoue K, Kamada F, Kure S, Goto Y, Japanese Mental Retardation Consortium. 2008. A loss-of-function mutation in the FTSJ1 gene causes nonsyndromic X-linked mental retardation in a Japanese family. Am J Med Genet Part B 147B:479–484.

Williams CA, Beaudet AL, Clayton-Smith J, Knoll JH, Kyllerman M, Laan LA, Magenis RE, Moncla A, Schinzel AA, Summers JA, Wagstaff J. 2006. Angelman Syndrome 2005: Updated consensus for diagnostic criteria. Am J Med Genet Part A 140A:413–418.

Molecular Genetics and Metabolism xxx (2012) xxx–xxx

Contents lists available at SciVerse ScienceDirect

Molecular Genetics and Metabolism

journal homepage: www.elsevier.com/locate/ymgme

Simple and rapid genetic testing for citrin deficiency by screening 11 prevalent mutations in *SLC25A13*

Atsuo Kikuchi [a,*], Natsuko Arai-Ichinoi [a], Osamu Sakamoto [a], Yoichi Matsubara [b], Takeyori Saheki [c,1], Keiko Kobayashi [d], Toshihro Ohura [e], Shigeo Kure [a]

[a] Department of Pediatrics, Tohoku University Graduate School of Medicine, 1-1 Seiryo-machi, Aoba-ku, Sendai, Miyagi 980-8574, Japan
[b] Department of Medical Genetics, Tohoku University School of Medicine, 1-1 Seiryo-machi, Aoba-ku, Sendai, Miyagi 980-8574, Japan
[c] Institute for Health Sciences, Tokushima Bunri University, 180 Yamashiro-cho, Tokushima 770-8514, Japan
[d] Department of Molecular Metabolism and Biochemical Genetics, Kagoshima University, Kagoshima 890-8544, Japan
[e] Division of Pediatrics, Sendai City Hospital, 3-1 Shimizukoji, Wakabayashi-ku, Sendai, Miyagi 984-8501, Japan

ARTICLE INFO

Article history:
Received 13 November 2011
Received in revised form 29 December 2011
Accepted 30 December 2011
Available online xxxx

Keywords:
Citrin deficiency
Genetic diagnosis
Rapid diagnosis
Expanded newborn screening
SLC25A13

ABSTRACT

Citrin deficiency is an autosomal recessive disorder caused by mutations in the *SLC25A13* gene and has two disease outcomes: adult-onset type II citrullinemia and neonatal intrahepatic cholestasis caused by citrin deficiency. The clinical appearance of these diseases is variable, ranging from almost no symptoms to coma, brain edema, and severe liver failure. Genetic testing for *SLC25A13* mutations is essential for the diagnosis of citrin deficiency because chemical diagnoses are prohibitively difficult. Eleven *SLC25A13* mutations account for 95% of the mutant alleles in Japanese patients with citrin deficiency. Therefore, a simple test for these mutations is desirable. We established a 1-hour, closed-tube assay for the 11 *SLC25A13* mutations using real-time PCR. Each mutation site was amplified by PCR followed by a melting-curve analysis with adjacent hybridization probes (HybProbe, Roche). The 11 prevalent mutations were detected in seven PCR reactions. Six reactions were used to detect a single mutation each, and one reaction was used to detect five mutations that are clustered in a 21-bp region in exon 17. To test the reliability, we used this method to genotype blind DNA samples from 50 patients with citrin deficiency. Our results were in complete agreement those obtained using previously established methods. Furthermore, the mutations could be detected without difficulty using dried blood samples collected on filter paper. Therefore, this assay could be used for newborn screening and for facilitating the genetic diagnosis of citrin deficiency, especially in East Asian populations.

1. Introduction

Citrin deficiency is an autosomal recessive disorder that results from mutations in the *SLC25A13* gene [1] and causes two diseases: adult-onset type II citrullinemia (CTLN2; OMIM #603471) and neonatal intrahepatic cholestasis caused by citrin deficiency (NICCD; OMIM#605814) [1–4]. The clinical appearance of these diseases is variable and ranges from almost no symptoms to coma, brain edema, and severe liver failure requiring transplantation [5–8]. In a study of patients with NICCD, only 40% of individuals were identified by newborn screenings to have abnormalities, such as hypergalactosemia, hypermethioninemia, and hyperphenylalaninemia [9]. Other patients were referred to hospitals with suspected neonatal hepatitis or biliary atresia, due to jaundice or discolored stool [9]. Hypercitrullinemia was not observed in all patients [9]. Mutation analysis of *SLC25A13* is indispensable because of the difficulties associated with the chemical diagnosis of citrin deficiency. The *SLC25A13* mutation spectrum in citrin deficiency is heterogeneous, and more than 31 mutations of *SLC25A13* have been identified to date [1,10–18]. However, there are several predominant mutations in patients from East Asia. As shown in Table 1, 6 prevalent mutations account for 91% of the mutant alleles in the Japanese population [12,19]. Five additional mutations also occur within a 21-bp cluster in exon 17 (Table 1 and Fig. 1D). The six prevalent mutations, together with the five mutations in exon 17, account for 95% of the mutant alleles in Japan [12,19].

Several different methods, such as direct sequencing, PCR restriction fragment length polymorphism (PCR-RFLP), and denaturing high performance liquid chromatography (DHPLC), are currently used for the detection of mutations in *SLC25A13* [1,10–14,19]. However, these methods are too complex for clinical use. Direct sequencing is a standard but cumbersome method. The PCR-RFLP method is

Abbreviations: CTLN2, adult-onset type II citrullinemia; FRET, fluorescence resonance energy transfer; HRM, high resolution melting; NICCD, neonatal intrahepatic cholestasis caused by citrin deficiency; Tm, melting temperature.

* Corresponding author. Fax: +81 22 717 7290.
E-mail address: akikuchi-thk@umin.ac.jp (A. Kikuchi).
[1] Present address: Institute of Resource Development and Analysis, Kumamoto University, Kumamoto 860-0811, Japan.

1096-7192/$ – see front matter © 2012 Elsevier Inc. All rights reserved.
doi:10.1016/j.ymgme.2011.12.024

Please cite this article as: A. Kikuchi, et al., Simple and rapid genetic testing for citrin deficiency by screening 11 prevalent mutations in *SLC25A13*, Mol. Genet. Metab. (2012), doi:10.1016/j.ymgme.2011.12.024

Table 1
Seven primer/probe sets and 11 targeted mutations of *SLC25A13*.

Primer/probe set	Mutation		Location	Nucleotide change	Effects of mutations	Allele frequency* [19]	References
A	Mutation [I]	:851del4	exon 9	c.851_854delGTAT	p.R284fs(286X)	33.2%	[1]
B	Mutation [II]	:g.IVS11+1G>A	intron 11	c.1019_1177del	p.340_392del	37.6%	[1]
C	Mutation [III]	:1638ins23	exon 16	c.1638_1660dup	p.A554fs(570X)	3.4%	[1]
D	Mutation [IV]	:S225X	exon 7	c.675C>A	p.S225X	5.3%	[1]
E	Mutation [V]	:g.IVS13+1G>A	intron 13	c.1231_1311del	p.411_437del	8.2%	[1]
F	Mutation [XIX]	:IVS16ins3kb	intron 16	c. aberrant RNA	p.A584fs(585X)	4.6%	[19]
G	Mutation [VI]	:1800ins1	exon 17	c.1799_1800insA	p.Y600X	1.3%	[10]
	Mutation [VII]	:R605X	exon 17	c.1813C>T	p.R605X	0.90%	[10]
	Mutation [VIII]	:E601X	exon 17	c.1801G>T	p.E601X	1.2%	[11]
	Mutation [IX]	:E601K	exon 17	c.1801G>A	p.E601K	0.30%	[11]
	Mutation [XXI]	:L598R	exon 17	c.1793T>G	p.L598R	0%	[15]
						Total 95.1%	

* The frequency of each mutant allele among Japanese patients with citrin deficiency.

complicated and can lead to genotyping errors, due to incomplete digestion by the restriction enzymes. DHPLC is time-consuming and requires expensive equipment. Thus, there is a strong need for the development of a simple test for these mutations.

The goal of this study was to establish a rapid and simple test for the detection of the 11 most common *SLC25A13* mutations. We adopted the HybProbe format (Roche) for the detection of the mutations using real-time PCR followed by a melting-curve analysis with adjacent hybridization probes [20,21]. This assay can be completed in less than 1 h and has the advantage of being a closed-tube assay. The fundamental process for detecting point mutations using the HybProbe assay is presented in Fig. 1A. The 11 prevalent mutations contain not only point mutations but also include a 4-bp deletion and insertions of 1-bp, 23-bp and 3-kb genomic fragments (Table 1 and Fig. 1). Careful design of the PCR primers and HybProbes enabled us to test for these various *SLC25A13* mutations.

2. Methods

2.1. Subjects

CTLN2 and NICCD were diagnosed, as previously described [9,10,19,22–24]. Genomic DNA of the patients was obtained from peripheral blood leukocytes using the DNeasy blood kit (Qiagen Inc., Valencia, CA, USA). Genomic DNA was purified from filter paper blood samples using the ReadyAmp Genomic DNA Purification System (Promega, Madison, WI, USA). Mutations in these DNA samples were analyzed at Kagoshima University using a combination of PCR with or without restriction enzyme digestion or by direct sequencing, as previously described [1,10–14,19]. Another set of samples was obtained from 420 healthy volunteers (mainly from Miyagi prefecture in the northeastern region of Japan) at Tohoku University. Genomic DNA from leukocytes was extracted, as described above.

2.2. Detection of seven prevalent mutations in SLC25A13 using the HybProbe assay

HybProbe probes comprise a pair of donor and acceptor oligonucleotide probes designed to hybridize adjacent to their target sites in an amplified DNA fragment [20,21]. The donor probes are labeled at their 3′ end with fluorescein isothiocyanate (FITC), whereas the acceptor probes are labeled at their 5′ end with LC Red640; these acceptor probes are phosphorylated at their 3′ end to prevent extension by the DNA polymerase. When two probes hybridize to the amplicon, the fluorescent dyes are located within 5 bases of each other, which allows fluorescence resonance energy transfer (FRET) between the excited FITC and the LC Red640; this process emits light that can be quantified by real-time PCR. Following PCR amplification, a melting-peak analysis is performed. The melting peak is produced by the reporter probe, which has a lower melting temperature (Tm) than the other probe, called the anchor probe. As the reporter melts from the target, the fluorophores are separated, and the FRET ceases. The Tm of the reporter probe determines the reaction

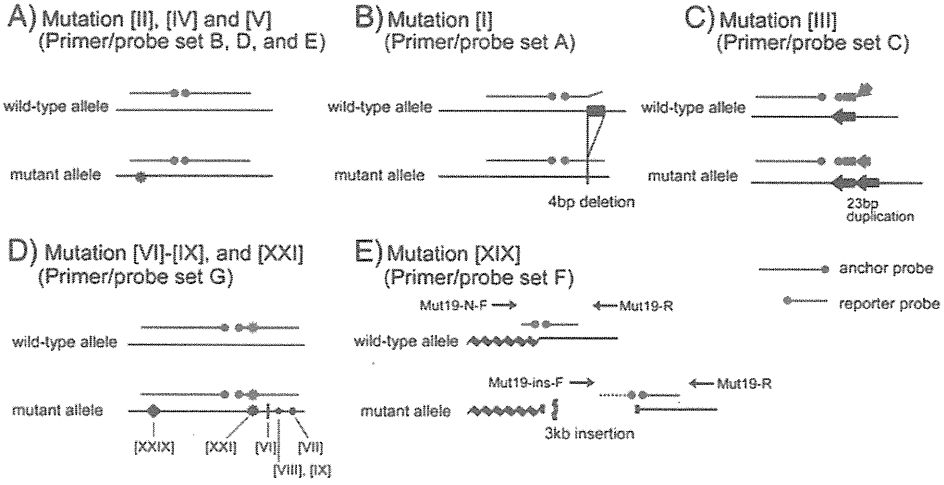

Fig. 1. Principle of *SLC25A13* mutation detection by melting-curve analysis with the HybProbe assay. In primer/probe sets A–E, and G, PCR was performed with a pair of primers, whereas in primer/probe set F, two forward primers and one common reverse primer were used for the amplification of both wild-type and mutant alleles. Note that mutation [XXIX], located on the anchor probe of primer/probe set G, is a non-target mutation.

Please cite this article as: A. Kikuchi, et al., Simple and rapid genetic testing for citrin deficiency by screening 11 prevalent mutations in *SLC25A13*, Mol. Genet. Metab. (2012), doi:10.1016/j.ymgme.2011.12.024

specificity (i.e., binding of the probe to a perfectly matched sequence rather than to regions with sequence mismatches).

Seven primer/probe sets were designed for this study. Fig. 1 shows a schematic diagram of the strategy for mutation detection using these primer/probe sets. Tables 1 and 2 list the primer/probe sets and corresponding sequences and primer concentrations that were used to target the 11 mutations. Primer/probe sets A, B, C, D, E, and F were designed to detect mutations [I], [II], [III], [IV], [V], and [XIX], respectively. Primer/probe set G was designed to detect the five mutations clustered on exon 17: mutations [VI], [VII], [VIII], [IX], and [XXI] (Fig. 1D). All primers and probes were synthesized based on the NCBI reference SLC25A13 gene sequence (GenBank accession no. **NM_014251**) with the exception of mutation [XIX]:IVS16ins3kb, which was designed according to [19].

Real-time PCR and subsequent melting curve analyses were performed in a closed tube using a 20-μL mixture on a LightCycler 1.5 (Roche Diagnostics, Tokyo, Japan). The PCR mixture contained 2.0 μL of genomic DNA (10–50 ng), 0.5 μM of forward primer, 0.5 or 0.1 μM of reverse primer, 0.2 μM of each sensor and anchor probe, and 10 μL of Premix ExTaq™ (Perfect Real Time) reagent (TaKaRa Bio Inc., Otsu, Japan).

The thermal profile conditions were identical for all seven assays and consisted of an initial denaturation step (30 s at 95 °C), followed by 45 amplification cycles with the following conditions: denaturation for 5 s at 95 °C and annealing and extension for 20 s at 60 °C. The transition rate between all steps was 20 °C/s. After amplification, the samples were held at 37 °C for 1 min, followed by the melting curve acquisition at a ramp rate of 0.15 °C/s extending to 80 °C with continuous fluorescence acquisition.

Table 2
Primers, probes and target amplicon sequences, target mutation sites, and primer concentrations.

Primer/probe set	Name	Sequences of PCR products, primer locations, probe sequences, and mutation sites (5′ to 3′)	Concentration (μmol/L)
A		GGCTATACTGAAATATGAGAAatgaaaaaagggatgtttttaaattttataatgtaaattgtaataaattggtatatttgttgcttgtgtttgtttttcccctacagac	
		gtatgaccttagcagacattgaacggattgctcctctggaagagggaactctgccCTTTAACTTGGCTGAGG (181 bp)	
	Mut1-F	GGCTATACTGAAATATGAGAA	0.5
	Mut1-R	CCTCAGCCAAGTTAAAG	0.5
	Mut1-UP	ATGTAAATTGTAATAAATTGGTATATTTGTTGCTTGTGTT-FITC	
	Mut1-DW	LC Red640-GTTTTTCCCCTACAGAC**GACC**-P	
B		GAATGCAGAACCAACGAtcaactggctcttttgtgggagaactcatgtataaaaacagctttgactgttttaagaaagtgctacgctatgaaggcttctt	
		tggactgtatagaggttagtgccacatgctcaatacctgttaggtgaaataacactcaaaggtttggtttctcatcttagtgcctGACATGAATTAGCAAGACTG (205 bp)	
	Mut2-F	GAATGCAGAACCAACGA	0.5
	Mut2-R	CAGTCTTGCTAATTCATGTC	0.1
	Mut2-UP	ACCTAACAGGTATTGAGCATGTG-FITC	
	MUt2-DW	LC Red640-CACTAACCTCTATACAGTCCA-P	
C		GCAGTTCAAAGCACAGTTATTtttatatagtgagaatgtgaccagactgagatggtgttgtgtctctcctgcaggtatgcctgcagcatctttagtg	
		accccctgctgatgttatcaagacgagattacaggtg	
		gctgcccggg(**gagatta**caggtggctgcccggg)ctggccaaaccaCTTACAGCGGAGTGATAGAC (175 bp)	
	Mut3-F	GCAGTTCAAAGCACAGTTATT	0.5
	Mut3-R	GTCTATCACTCCGCTGTAAG	0.5
	Mut3-UP	ACCCCTGCTGATGTTATCAAGACGAGATTACAGGT-FITC	
	Mut3-DW	LC Red640-GCTGCCCGGG**GAGATTA**-P	
D		TCAATTTATTTGAGGCTGCtggaggtaccacatcccatcaagttagtttctcctattttaatggatttaattcgctccttaacaac	
		atggaactcattagaaagatctatagcactc	
		tggctggcaccaggaaagatgttgaagtGACTAAGGGTGAGTGAGAA (164 bp)	
	Mut4-F	TCAATTTATTTGAGGCTGC	0.5
	Mut4-R	TTCTCACTCACCCTTAGTC	0.5
	Mut4-UP	AATGGATTTAATT**C**GCTCCTTAACA-FITC	
	Mut4-DW	LC Red640-ATGGAACTCATTAGAAAGATCTATAGCACTC-P	
E		TGCACAAAGATGGTTCGgtcccacttgcagcagaaattcttgctggaggctgcgtaagtacctttgaagctctcttcattgaaaagacttgtttcac	
		atatatatcactaccatggtcaacaggtgtggactaaggcttctgttTAACCACAGATCCTGCA (162 bp)	
	Mut5-F	TGCACAAAGATGGTTCG	0.5
	Mut5-R	TGCAGGATCTGTGGTTA	0.5
	Mut5-UP	GTGAAACAAGTCTTTTCAATGAAGAGAGCTTC-FITC	
	Mut5-DW	LC Red640-AAGGTACTTA**C**GCAGCCTC-P	
F	normal allele	GGAGCTGGTGGTATGGAAataatgtgttcttaactaactctttggtatcaggtaaatttttaaaatatctaattatatctgtgatttctc	
		catttttttaaagctcgtgtatttcgatcctcaccccagtttggt	
		gtaactttgctgacttacgaattgctacagcgatggttctacattgattttggaggagtgtaagtatcatgctaaatctgctgctaaatttt	
		GGCTGCTGCTAATGCTC (244 bp)	
	insertion allele	CCATCTTCCTCCTCCCTTggcagccccgccccccgatttctccatttttttaaagctcgtgtatttcgatcctcaccccagtttggt	
		gtaactttgctgacttacgaattgctacagcgatggttctacattgatttt	
		ggaggagtgtaagtatcatgctaaatctgctgctaaatttGGCTGCTGCTAATGCTC (196 bp)	
	Mut19-N-F	GGAGCTGGTGGTATGGAA	0.5
	Mut19-ins-F	CCATCTTCCTCCTCCCTT	0.5
	Mut19-R	GAGCATTAGCAGCAGCC	0.5
	Mut19-UP	ACCAAACTGGGGTGAGGATCGAAATACACGAGCTTTAAAAAAATG-FITC	
	Mut19-N-DW	LC Red640-AGAAATCACAGATATAATTAGATATTT-P	
	Mut19-ins-DW	LC Red640-AGAAATCGGGGGGCGGGG-P	
G		TCTTAACTAACTCTTTGGTATCAGGTaaatttttaaaatatctaattatatctgtgatttctccatttttttaaagctcg	
		tgtatttcgatcctcaccccagtttggtgtaactttgctgactta(a)cgaattgctacagcga	
		tggttctacattgattttggaggagtgtaagtatcatgctaaatctgctgctaaatttGGCTGCTGCTAATGCTC (217 bp)	
	Mut6-9, 21-F	TCTTAACTAACTCTTTGGTATCAGGT	0.5
	Mut6-9, 21-R	GAGCATTAGCAGCAGCC	0.5
	Mut6-9, 21-UP	TGTATTTCGATCCTCACCCCAGTTTGGTGTAACTT-FITC	
	Mut6-9, 21-DW	LC Red640-GC**GGACTTACG**AATTGCTACAG**C**GA-P	

Upper case and underlined letters indicate the locations of primers and probes, respectively. Inserted DNA is shown in parenthesis. Nucleotides in boldface were used for mutation detection.
F: forward, R: reverse, UP: upstream, DW: downstream, N: normal allele, ins: insertion allele, FITC: fluorescein isothiocyanate, P: phosphate.

Please cite this article as: A. Kikuchi, et al., Simple and rapid genetic testing for citrin deficiency by screening 11 prevalent mutations in *SLC25A13*, Mol. Genet. Metab. (2012), doi:10.1016/j.ymgme.2011.12.024

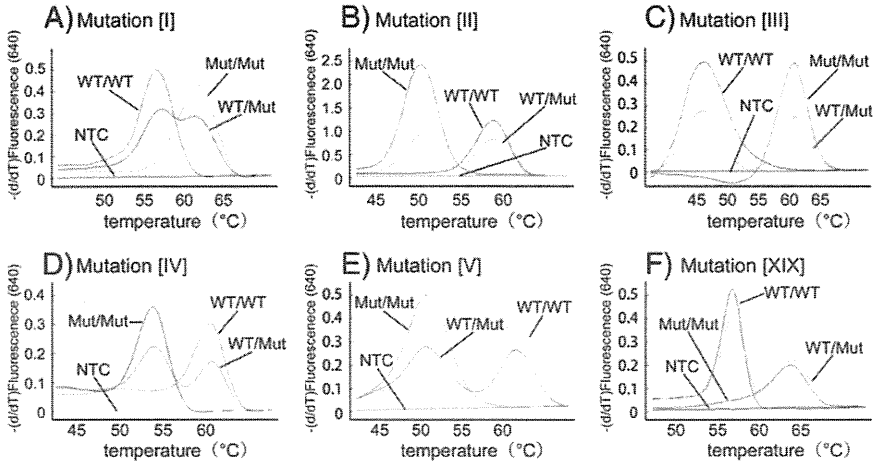

Fig. 2. Typical melting curves used in the detection of mutations [I–V] and [XIX]. Each assay using primer/probe sets A–F is displayed in a separate graph (A–F). WT: wild-type allele, Mut: mutant allele, NTC: no DNA template control.

2.3. Validation of the mutation detection system

After establishing the protocol for detecting the 11 prevalent mutations, 50 DNA samples from patients' blood were sent from Kagoshima University to Tohoku University for the validation of this system in a single-blind manner. Similarly, 26 DNA samples purified from paper-filter blood samples were analyzed in the same manner as the blood DNA samples.

2.4. Estimation of the carrier frequency

For the estimation of the heterozygous carrier frequency, 420 genomic DNA samples from healthy volunteers were screened using the HybProbe analysis for the 11 prevalent mutations. All detected mutations were confirmed by direct sequencing.

2.5. Ethics

This study was approved by the Ethical Committees of Tohoku University School of Medicine and Kagoshima University. Written informed consent was obtained from all participants or their guardians.

3. Results

3.1. Development of the mutation detection system

In primer/probe sets B, D, and E, the reporter probes were designed to be complimentary to the wild-type allele (Fig. 1A). To allow for an improved detection of the mutations, primer/probe sets A and C were designed to be complementary to the mutant allele (Figs. 1B, C). In the primer/probe set F, two forward PCR primers, which were specific to the wild-type and the mutant alleles, were used with a common reverse primer for the co-amplification of the wild-type and 3-kb insertion alleles (Fig. 1E). Two reporter probes, which had a common anchor probe, were used for the detection of the wild-type and mutant alleles. Because the two reporter probes had different melting temperatures, we were able to identify the allele that was amplified. Fig. 2 shows representative results of the melting curve analyses using the primer/probe sets A–F, in which all of the mutant alleles generated distinct peaks corresponding to the wild-type alleles.

In the primer/probe set G, we used a reporter probe that was complementary to the mutant [XXI] allele (Fig. 1D). All five mutations in exon 17 were successfully differentiated from the wild-type allele (Figs. 3A–E). The [XXIX] mutation is an additional mutation in exon

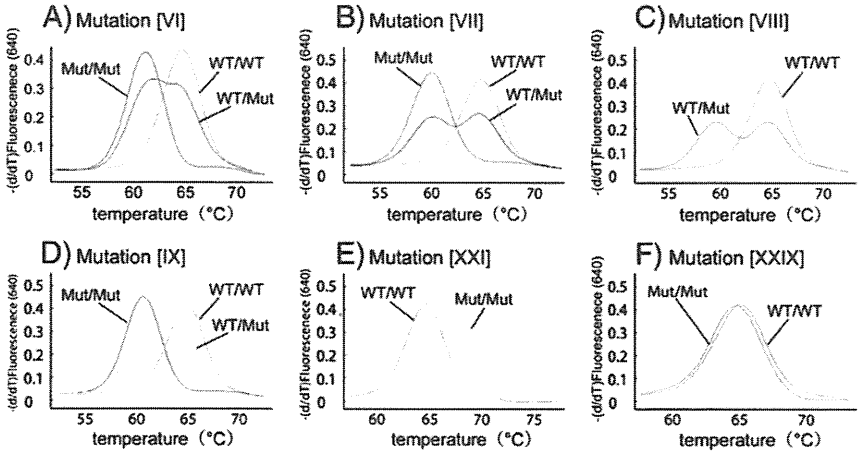

Fig. 3. Typical melting curves used in the detection of mutations [VI–XI], [XXI], and [XXIX] on exon 17. Genotyping was performed using primer/probe set G. Each melting curve for a target mutation is displayed in a separate graph (A–F). Note that mutation [XXIX] (F) is a non-target mutation on the anchor probe. WT: wild-type allele, Mut: mutant allele.

Please cite this article as: A. Kikuchi, et al., Simple and rapid genetic testing for citrin deficiency by screening 11 prevalent mutations in *SLC25A13*, Mol. Genet. Metab. (2012), doi:10.1016/j.ymgme.2011.12.024

17 that is not listed in Table 1. The [XXIX] mutation is located in the anchor-probe binding site and not on the reporter-probe binding site (Fig. 1D). To examine the effect of mutations on the anchor probe, we genotyped a patient with a heterozygous [XXIX] mutation using primer/probe set G (Fig. 3F). We found no change in the melting curves between the wild-type allele and the [XXIX] allele, thereby suggesting that point mutations within the anchor probe sequence have little effect on the melting curve analysis.

3.2. Validation

The genotypes determined at Tohoku University using the proposed method and those determined at Kagoshima University using a previously published method were identical for the 11 common mutations (Table S1 in supplementary material). We performed a similar test using DNA samples purified from filter-paper blood samples to determine if this method could be used for newborn screening. The genotypes determined in both laboratories were identical for all 26 DNA samples (Table S2 in supplementary material).

3.3. Frequency of eleven prevalent mutations

We found four heterozygous carriers of mutation [I], three of mutation [II], and two of mutation [V]. In addition, primer/probe set G detected one heterozygous mutation, which was confirmed as mutation [VIII] by direct sequencing. Altogether, 10 mutations were detected in 420 Japanese healthy controls.

4. Discussion

We developed a simple and rapid genetic test using real-time PCR combined with the HybProbe system for the 11 prevalent mutations in *SLC25A13*: mutations [I], [II], [III], [IV], [V], [VI], [VII], [VIII], [IX], [XIX], and [XXI]. This genetic test is a closed-tube assay in which no post-PCR handling of the samples is required. In addition, the genotyping is completed within 1 h. This test can utilize DNA samples purified from both peripheral blood and filter-paper blood. The reliability of the test was confirmed by genotyping 76 blind DNA samples from patients with citrin deficiency, including 50 peripheral blood and 26 filter-paper blood DNA samples. Because screening for the 11 targeted mutations would identify 95% of mutant alleles in the Japanese population [19], both, one, and no mutant alleles are expected to be identified in 90.4%, 9.3%, and less than 0.3% of patients, respectively. This genetic test would be useful not only in Japan but also other East Asian countries, including China, Korea, Taiwan and Vietnam, in which the same mutations are prevalent. Our test is expected to detect 76–87% of the mutant alleles in the Chinese population [12,19,25], 95–100% in the Korean population [12,19,26], 60–68% in the Taiwanese population [27,28], and 100% in the Vietnamese population [12,19]. If we were to prepare a primer/probe set for mutation [X]:g.IVS6+5G>A [12], which is prevalent in Taiwan, the estimated sensitivity would exceed 90% in the Taiwanese population [27,28].

Recently, the high resolution melting (HRM) method was reported to be suitable for the screening of mutations in the diagnosis of citrin deficiency [28]. HRM analysis is a closed-tube assay that screens for any base changes in the amplicons. The presence of SNPs anywhere on the amplicons can affect the melting curve, thereby suggesting that HRM is not suitable for screening for known mutations, but rather, is best suited to screening for unknown mutations. When we detected one heterozygous prevalent mutation, we performed HRM screening for all 17 exons of *SLC25A13*. After HRM screening, only the HRM-positive exons were subjected to direct sequencing analysis. Several mutant alleles were identified using this approach.

The frequency of homozygotes, including compound heterozygotes, presenting *SLC25A13* mutations in the population at Kagoshima (a prefecture in the southern part of Japan) has been calculated to be 1/17,000 based on the carrier rate (1/65) [19]. The prevalence of NICCD has been also reported to be 1/17,000–34,000 [29]. In this study, the carrier rate in Miyagi (a prefecture in northern Japan) was 1/42 (95% confidential interval, 1/108–1/26), thereby yielding an estimated frequency of patients with citrin deficiency of 1/7,100. Our result, together with the previous report [19], suggests that a substantial fraction of the homozygotes or compound heterozygotes of SLC25A13 mutations was asymptomatic during the neonatal period.

The early and definitive diagnosis of citrin deficiency may be beneficial for patients with citrin deficiency by encouraging specific dietary habits and avoiding iatrogenic worsening of brain edema by glycerol infusion when patients develop encephalopathy [30,31]. Because the screening of blood citrulline levels by tandem mass analysis at birth does not detect all patients with citrin deficiency, the development of a genetic test would be welcomed. In this study, we demonstrated that genomic DNA extracted from filter paper blood samples was correctly genotyped, thereby indicating the feasibility of newborn screening using this genetic test. If 100,000 babies in the northern part of Japan were screened by this method, we would detect 14 homozygotes or compound heterozygotes with *SLC25A13* mutations and 2400 heterozygous carriers. In 2400 heterozygous carriers, we would expect to observe only 1 to 2 compound heterozygotes with one target and one non-target mutation. The estimated frequency of babies with two non-target mutations is 0.04/100,000. Our genetic method would therefore allow us to screen newborn babies efficiently. If we performed this genetic test in a high-throughput real-time PCR system, such as a 384- or 1,536-well format, the cost per sample could be lowered.

In conclusion, we have established a rapid and simple detection system using the HybProbe assay for the 11 prevalent mutations in *SLC25A13*. This system could be used to screen newborns for citrin deficiency and may facilitate the genetic diagnosis of citrin deficiency, especially in East Asian populations.

Supplementary materials related to this article can be found online at doi:10.1016/j.ymgme.2011.12.024.

Acknowledgments

The authors acknowledge the contribution of Dr. Keiko Kobayashi, who passed away on December 21th, 2010. Dr. Kobayashi discovered that the *SLC25A13* gene is responsible for citrin deficiency and devoted much of her life to elucidating the mechanism of citrin deficiency. This work was supported by grants from the Ministry of Education, Culture, Sports, Science, and Technology and the Ministry of Health, Labor, and Public Welfare.

References

[1] K. Kobayashi, D.S. Sinasac, M. Iijima, A.P. Boright, L. Begum, J.R. Lee, T. Yasuda, S. Ikeda, R. Hirano, H. Terazono, M.A. Crackower, I. Kondo, L.C. Tsui, S.W. Scherer, T. Saheki, The gene mutated in adult-onset type II citrullinaemia encodes a putative mitochondrial carrier protein, Nat. Genet. 22 (1999) 159–163.
[2] T. Ohura, K. Kobayashi, Y. Tazawa, I. Nishi, D. Abukawa, O. Sakamoto, K. Iinuma, T. Saheki, Neonatal presentation of adult-onset type II citrullinemia, Hum. Genet. 108 (2001) 87–90.
[3] Y. Tazawa, K. Kobayashi, T. Ohura, D. Abukawa, F. Nishinomiya, Y. Hosoda, M. Yamashita, I. Nagata, Y. Kono, T. Yasuda, N. Yamaguchi, T. Saheki, Infantile cholestatic jaundice associated with adult-onset type II citrullinemia, J. Pediatr. 138 (2001) 735–740.
[4] T. Tomomasa, K. Kobayashi, H. Kaneko, H. Shimura, T. Fukusato, M. Tabata, Y. Inoue, S. Ohwada, M. Kasahara, Y. Morishita, M. Kimura, T. Saheki, A. Morikawa, Possible clinical and histologic manifestations of adult-onset type II citrullinemia in early infancy, J. Pediatr. 138 (2001) 741–743.
[5] T. Shigeta, M. Kasahara, T. Kimura, A. Fukuda, K. Sasaki, K. Arai, A. Nakagawa, S. Nakagawa, K. Kobayashi, S. Soneda, H. Kitagawa, Liver transplantation for an

Please cite this article as: A. Kikuchi, et al., Simple and rapid genetic testing for citrin deficiency by screening 11 prevalent mutations in *SLC25A13*, Mol. Genet. Metab. (2012), doi:10.1016/j.ymgme.2011.12.024

infant with neonatal intrahepatic cholestasis caused by citrin deficiency using heterozygote living donor, Pediatr. Transplant. 14 (2009) E86–88.
[6] M. Kasahara, S. Ohwada, T. Takeichi, H. Kaneko, T. Tomomasa, A. Morikawa, K. Yonemura, K. Asonuma, K. Tanaka, K. Kobayashi, T. Saheki, I. Takeyoshi, Y. Morishita, Living-related liver transplantation for type II citrullinemia using a graft from heterozygote donor, Transplantation 71 (2001) 157–159.
[7] Y. Takashima, M. Koide, H. Fukunaga, M. Iwai, M. Miura, R. Yoneda, T. Fukuda, K. Kobayashi, T. Saheki, Recovery from marked altered consciousness in a patient with adult-onset type II citrullinemia diagnosed by DNA analysis and treated with a living related partial liver transplantation, Intern. Med. 41 (2002) 555–560.
[8] A. Tamamori, Y. Okano, H. Ozaki, A. Fujimoto, M. Kajiwara, K. Fukuda, K. Kobayashi, T. Saheki, Y. Tagami, T. Yamano, Neonatal intrahepatic cholestasis caused by citrin deficiency: severe hepatic dysfunction in an infant requiring liver transplantation, Eur. J. Pediatr. 161 (2002) 609–613.
[9] T. Ohura, K. Kobayashi, Y. Tazawa, D. Abukawa, O. Sakamoto, S. Tsuchiya, T. Saheki, Clinical pictures of 75 patients with neonatal intrahepatic cholestasis caused by citrin deficiency (NICCD), J. Inherit. Metab. Dis. 30 (2007) 139–144.
[10] T. Yasuda, N. Yamaguchi, K. Kobayashi, I. Nishi, H. Horinouchi, M.A. Jalil, M.X. Li, M. Ushikai, M. Iijima, I. Kondo, T. Saheki, Identification of two novel mutations in the SLC25A13 gene and detection of seven mutations in 102 patients with adult-onset type II citrullinemia, Hum. Genet. 107 (2000) 537–545.
[11] N. Yamaguchi, K. Kobayashi, T. Yasuda, I. Nishi, M. Iijima, M. Nakagawa, M. Osame, I. Kondo, T. Saheki, Screening of SLC25A13 mutations in early and late onset patients with citrin deficiency and in the Japanese population: identification of two novel mutations and establishment of multiple DNA diagnosis methods for nine mutations, Hum. Mutat. 19 (2002) 122–130.
[12] Y.B. Lu, K. Kobayashi, M. Ushikai, A. Tabata, M. Iijima, M.X. Li, L. Lei, K. Kawabe, S. Taura, Y. Yang, T.-T. Liu, S.-H. Chiang, K.-J. Hsiao, Y.-L. Lau, L.-C. Tsui, D.H. Lee, T. Saheki, Frequency and distribution in East Asia of 12 mutations identified in the SLC25A13 gene of Japanese patients with citrin deficiency, J. Hum. Genet. 50 (2005) 338–346.
[13] E. Ben-Shalom, K. Kobayashi, A. Shaag, T. Yasuda, H.-Z. Gao, T. Saheki, C. Bachmann, O. Elpeleg, Infantile citrullinemia caused by citrin deficiency with increased dibasic amino acids, Mol. Genet. Metab. 77 (2002) 202–208.
[14] J. Takaya, K. Kobayashi, A. Ohashi, M. Ushikai, A. Tabata, S. Fujimoto, F. Yamato, T. Saheki, Y. Kobayashi, Variant clinical courses of 2 patients with neonatal intrahepatic cholestasis who have a novel mutation of SLC25A13, Metab. Clin. Exp. 54 (2005) 1615–1619.
[15] A. Luder, A. Tabata, M. Iijima, K. Kobayashi, H. Mandel, Citrullinaemia type 2 outside East Asia: Israeli experience, J. Inherit. Metab. Dis. 29 (2006) 59.
[16] T. Hutchin, M. Preece, K. Kobayashi, T. Saheki, R. Brown, D. Kelly, P. McKiernan, A. Green, U. Baumann, Neonatal intrahepatic cholestasis caused by citirn deficiency (NICCD) in a European patient, J. Inherit. Metab. Dis. 29 (2006) 112.
[17] J.-S. Sheng, M. Ushikai, M. Iijima, S. Packman, K. Weisiger, M. Martin, M. McCracken, T. Saheki, K. Kobayashi, Identification of a novel mutation in a Taiwanese patient with citrin deficiency, J. Inherit. Metab. Dis. 29 (2006) 163.
[18] J.M. Ko, G.-H. Kim, J.-H. Kim, J.Y. Kim, J.-H. Choi, M. Ushikai, T. Saheki, K. Kobayashi, H.-W. Yoo, Six cases of citrin deficiency in Korea, Int. J. Mol. Med. 20 (2007) 809–815.
[19] A. Tabata, J.-S. Sheng, M. Ushikai, Y.-Z. Song, H.-Z. Gao, Y.-B. Lu, F. Okumura, M. Iijima, K. Mutoh, S. Kishida, T. Saheki, K. Kobayashi, Identification of 13 novel mutations including a retrotransposal insertion in SLC25A13 gene and frequency of 30 mutations found in patients with citrin deficiency, J. Hum. Genet. 53 (2008) 534–545.
[20] P.S. Bernard, R.S. Ajioka, J.P. Kushner, C.T. Wittwer, Homogeneous multiplex genotyping of hemochromatosis mutations with fluorescent hybridization probes, Am. J. Pathol. 153 (1998) 1055–1061.
[21] C.N. Gundry, P.S. Bernard, M.G. Herrmann, G.H. Reed, C.T. Wittwer, Rapid F508del and F508C assay using fluorescent hybridization probes, Genet. Test. 3 (1999) 365–370.
[22] T. Saheki, K. Kobayashi, I. Inoue, Hereditary disorders of the urea cycle in man: biochemical and molecular approaches, Rev. Physiol. Biochem. Pharmacol. 108 (1987) 21–68.
[23] K. Kobayashi, M. Horiuchi, T. Saheki, Pancreatic secretory trypsin inhibitor as a diagnostic marker for adult-onset type II citrullinemia, Hepatology 25 (1997) 1160–1165.
[24] Y. Tazawa, K. Kobayashi, D. Abukawa, I. Nagata, S. Maisawa, R. Sumazaki, T. Iizuka, Y. Hosoda, M. Okamoto, J. Murakami, S. Kaji, A. Tabata, Y.B. Lu, O. Sakamoto, A. Matsui, S. Kanzaki, G. Takada, T. Saheki, K. Iinuma, T. Ohura, Clinical heterogeneity of neonatal intrahepatic cholestasis caused by citrin deficiency: case reports from 16 patients, Mol. Genet. Metab. 83 (2004) 213–219.
[25] H.Y. Fu, S.R. Zhang, X.H. Wang, T. Saheki, K. Kobayashi, J.S. Wang, The mutation spectrum of the SLC25A13 gene in Chinese infants with intrahepatic cholestasis and aminoacidemia, J. Gastroenterol. 46 (2011) 510–518.
[26] K. Kobayashi, Y.B. Lu, M.X. Li, I. Nishi, K.-J. Hsiao, K. Choeh, Y. Yang, W.-L. Hwu, J.K.V. Reichardt, F. Palmieri, Y. Okano, T. Saheki, Screening of nine SLC25A13 mutations: their frequency in patients with citrin deficiency and high carrier rates in Asian populations, Mol. Genet. Metab. 80 (2003) 356–359.
[27] T. Saheki, K. Kobayashi, M. Iijima, M. Horiuchi, L. Begum, M.A. Jalil, M.X. Li, Y.B. Lu, M. Ushikai, A. Tabata, M. Moriyama, K.-J. Hsiao, Y. Yang, Adult-onset type II citrullinemia and idiopathic neonatal hepatitis caused by citrin deficiency: involvement of the aspartate glutamate carrier for urea synthesis and maintenance of the urea cycle, Mol. Genet. Metab. 81 (Suppl 1) (2004) S20–S26.
[28] J.T. Lin, K.J. Hsiao, C.Y. Chen, C.C. Wu, S.J. Lin, Y.Y. Chou, S.C. Shiesh, High resolution melting analysis for the detection of SLC25A13 gene mutations in Taiwan, Clin. Chim. Acta 412 (2011) 460–465.
[29] Y. Shigematsu, S. Hirano, I. Hata, Y. Tanaka, M. Sudo, N. Sakura, T. Tajima, S. Yamaguchi, Newborn mass screening and selective screening using electrospray tandem mass spectrometry in Japan, J. Chromatogr. B Analyt. Technol. Biomed. Life Sci. 776 (2002) 39–48.
[30] M. Yazaki, Y.-i. Takei, K. Kobayashi, T. Saheki, S.-I. Ikeda, Risk of worsened encephalopathy after intravenous glycerol therapy in patients with adult-onset type II citrullinemia (CTLN2), Intern. Med. 44 (2005) 188–195.
[31] H. Takahashi, T. Kagawa, K. Kobayashi, H. Hirabayashi, M. Yui, L. Begum, T. Mine, S. Takagi, T. Saheki, Y. Shinohara, A case of adult-onset type II citrullinemia—deterioration of clinical course after infusion of hyperosmotic and high sugar solutions, Med. Sci. Monit. 12 (2006) CS13–CS15.

Please cite this article as: A. Kikuchi, et al., Simple and rapid genetic testing for citrin deficiency by screening 11 prevalent mutations in *SLC25A13*, Mol. Genet. Metab. (2012), doi:10.1016/j.ymgme.2011.12.024

HMG Advance Access published December 30, 2011

Human Molecular Genetics, 2011 **1–8**
doi:10.1093/hmg/ddr585

Mutations in genes encoding the glycine cleavage system predispose to neural tube defects in mice and humans

Ayumi Narisawa[1,2], Shoko Komatsuzaki[1], Atsuo Kikuchi[3], Tetsuya Niihori[1], Yoko Aoki[1], Kazuko Fujiwara[4], Mitsuyo Tanemura[5], Akira Hata[6], Yoichi Suzuki[6], Caroline L. Relton[7], James Grinham[8], Kit-Yi Leung[8], Darren Partridge[8], Alexis Robinson[8], Victoria Stone[8], Peter Gustavsson[9], Philip Stanier[8], Andrew J. Copp[8], Nicholas D.E. Greene[8,*], Teiji Tominaga[2], Yoichi Matsubara[1] and Shigeo Kure[1,3,*]

[1]Department of Medical Genetics, [2]Department of Neurosurgery and [3]Department of Pediatrics, Tohoku University School of Medicine, Sendai, Japan, [4]Institute for Enzyme Research, University of Tokushima, Tokushima, Japan, [5]Tanemura Women's Clinic, Nagoya, Japan, [6]Department of Public Health, Chiba University School of Medicine, Chiba, Japan, [7]Human Nutrition Research Centre, Institute for Ageing and Health, Newcastle University, Newcastle upon Tyne, UK, [8]Institute of Child Health, University College London, London, UK and [9]Department of Molecular Medicine and Surgery, Karolinska Institute, Stockholm, Sweden

Received October 26, 2011; Revised November 25, 2011; Accepted December 6, 2011

Neural tube defects (NTDs), including spina bifida and anencephaly, are common birth defects of the central nervous system. The complex multigenic causation of human NTDs, together with the large number of possible candidate genes, has hampered efforts to delineate their molecular basis. Function of folate one-carbon metabolism (FOCM) has been implicated as a key determinant of susceptibility to NTDs. The glycine cleavage system (GCS) is a multi-enzyme component of mitochondrial folate metabolism, and GCS-encoding genes therefore represent candidates for involvement in NTDs. To investigate this possibility, we sequenced the coding regions of the GCS genes: *AMT*, *GCSH* and *GLDC* in NTD patients and controls. Two unique non-synonymous changes were identified in the *AMT* gene that were absent from controls. We also identified a splice acceptor site mutation and five different non-synonymous variants in *GLDC*, which were found to significantly impair enzymatic activity and represent putative causative mutations. In order to functionally test the requirement for GCS activity in neural tube closure, we generated mice that lack GCS activity, through mutation of *AMT*. Homozygous *Amt*$^{-/-}$ mice developed NTDs at high frequency. Although these NTDs were not preventable by supplemental folic acid, there was a partial rescue by methionine. Overall, our findings suggest that loss-of-function mutations in GCS genes predispose to NTDs in mice and humans. These data highlight the importance of adequate function of mitochondrial folate metabolism in neural tube closure.

INTRODUCTION

Neural tube defects (NTDs), such as spina bifida and anencephaly, are severe birth defects that result from failure of closure of the neural folds during embryonic development (1). Although NTDs are among the commonest birth defects in humans, the causes are still not well understood. This is most likely due to their complex, multifactorial causation

*To whom correspondence should be addressed at: Neural Development Unit, UCL Institute of Child Health, Guilford Street, London, WC1N 1EH, UK. Email: n.greene@ucl.ac.uk (N.D.E.G.); Department of Pediatrics, Tohoku University School of Medicine, 1-1 Seiryomachi, Aobaku, Sendai 980-8574, Japan. Email: kure@med.tohoku.ac.jp (S.Ku.)

which is thought to involve contributions from both genetic and environmental factors (2–4). The potential complexity of NTD genetics is illustrated by the fact that more than 200 different genes give rise to NTDs when mutated in mice (5,6). Moreover, inheritance patterns in humans suggest a multigenic model in which an affected individual may carry two or more risk alleles, which by themselves may be insufficient to cause NTDs (2).

Folate one-carbon metabolism (FOCM) is strongly implicated as a determinant of susceptibility to NTDs since suboptimal maternal folate status and/or elevated homocysteine are established risk factors, whereas periconceptional maternal folic acid supplementation can reduce the occurrence and recurrence of NTDs (7,8). Nevertheless, the precise mechanism by which folate status influences NTD risk remains elusive (7,9). FOCM comprises a network of enzymatic reactions required for synthesis of purines and thymidylate for DNA synthesis, and methionine, which is required for methylation of biomolecules (Fig. 1A) (9). In addition to the cytosol, FOCM also operates in mitochondria, supplying extra one-carbon units to the cytosolic FOCM as formate (Fig. 1A) (10).

Genes that are functionally related to folate metabolism have been subjected to intensive genetic analysis in relation to NTD causation, principally through association studies (reviewed in 3,4,11). In the most extensively studied gene, *MTHFR*, the c.677C>T SNP is associated with NTDs in some, but not all, populations. However, other FOCM-related genes have largely shown non-significant or only mild associations. Given the apparently complex inheritance of the majority of human NTDs, many association studies have been hampered by limitations on sample size. Moreover, although positive associations have been noted for other genes including *DHFR*, *MTHFD1*, *MTRR* and *TYMS* (12,13), these have not been replicated in all populations, and additional studies are required. The hypothesis that genetically determined abnormalities of folate metabolism may contribute to NTD susceptibility is supported by the observation of defects of thymidylate biosynthesis in a proportion of primary cell lines derived from NTDs (14). However, these defects do not correspond with known polymorphisms in FOCM-related genes. Overall, it appears likely that genetic influences on folate metabolism remain to be identified in many NTDs.

A potential link between mitochondrial FOCM and NTDs was suggested by the finding of an association of increased NTD risk with an intronic polymorphism in *MTHFD1L* (15). Another component of mitochondrial FOCM, the glycine cleavage system (GCS), acts to break down glycine to donate one-carbon units to tetrahydrofolate (THF), generating 5,10-methylenetetrahydrofolate (methylene-THF; Fig. 1B) (16,17). The GCS consists of four enzyme components, each of which is required for the glycine cleavage reaction (18,19). The components—glycine dehydrogenase (decarboxylating) (GLDC; P-protein), aminomethlyltransferase (AMT; T-protein), glycine cleavage system protein H (GCSH; H-protein) and dihydrolipoamide dehydrogenase (DLD; L-protein)—are encoded by distinct genes: *GLDC*, *AMT*, *GCSH* and *DLD*, respectively. The functions of *GLDC*, *AMT* and *GCSH* are specific to the GCS, whereas *DLD* encodes a housekeeping enzyme. GCS components have been found to be abundantly expressed in the neuroepithelium during embryogenesis in the rat (20).

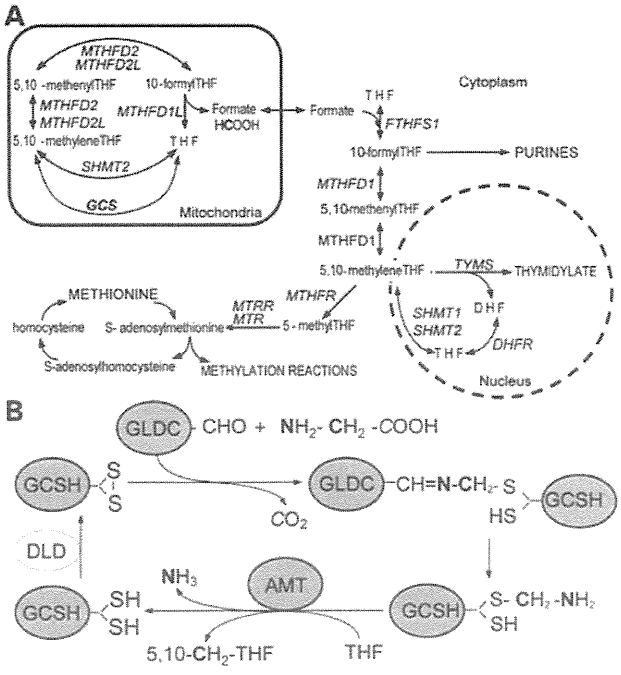

Figure 1. Schematic diagrams summarizing the key reactions of folate-mediated one-carbon metabolism and the GCS. (**A**) Folates donate and accept one-carbon units in the synthesis of purines, thymidylate and methionine. Mitochondrial FOCM supplies one-carbon units to the cytoplasm via formate. The GCS is a key component of mitochondrial FOCM that breaks down glycine and generates 5,10-methylene-THF from THF. Genes encoding enzymes for each reaction are indicated in italics. DHF, dihydrofolate; THF, tetrahydrofolate. (**B**) Summary of the GCS. The glycine cleavage reaction is catalysed by the sequential action of four individual enzymes: GLDC, GCSH, AMT and DLD. The first three of these (shaded grey) are specific to the GCS. Glycine is broken down into CO_2 and NH_3, and donates a one-carbon unit (indicated in bold) to THF, generating 5,10-methylene-THF. The other carbon in glycine (indicated in italics) enters CO_2.

We hypothesized that modulation of GCS activity has the potential to influence efficacy of cellular FOCM during the period of neural tube closure and, hence, susceptibility to NTDs. Therefore, in the current study, we screened genes encoding GCS components for possible mutations in NTD patients and controls. We tested variant proteins for loss of function by enzymatic assay and mice lacking GCS function were generated, to test the effect on embryonic development.

RESULTS

The hypothesis that genes of the GCS represent candidates for involvement in NTDs prompted us to screen for potential mutations in patient samples. Coding exons of *AMT* (9 exons), *GCSH* (5 exons) and *GLDC* (25 exons) were sequenced in a total of 258 NTD patients comprising cohorts from Japan, the UK and Sweden. Each of the major categories of NTDs was represented among study samples, including anencephaly ($n = 38$), spina bifida ($n = 198$) and craniorachischisis ($n = 22$).

Table 1. Nucleotide changes in NTD patients and controls identified by exon sequencing of AMT, GLDC and GCSH

Location	Nucleotide change	Effect	Number of mutation carriers in UK cohorts		Number of mutation carriers in the Japanese cohort		Number of mutation carriers in the Swedish cohort		Variant GLDC enzyme activity[a]
			NTD group (type[b]) ($n = 166$)[c]	Control group ($n = 189$)[c]	NTD group (type[b]) ($n = 14$)[c]	Control group ($n = 36$)[c]	NTD group (type[b]) ($n = 76$)[c]	Control group ($n = 145$)[c]	
AMT									
Exon 2	c.103A>C	p.R35R	0	1	0	0	0	—	
	c.214A>G	p.T72A	0	0	0	1	0	—	
Exon 6	c.623C>A	p.A208D	0	2	0	0	0	—	
	c.631G>A	p.E211K[d]	2 (SBA)	0	0	0	1	—	
	c.589G>C	p.D197H	0	0	1 (An)	0	0	—	
Exon 7	c.825T>A	p.N275K	0	1	0	0	0	—	
	c.850G>C	p.V284L	1 (SBA)	0	0	0	0	—	
GLDC									
Exon 1	c.52G>T	p.G18C	2 (SBO/SBA)	2	0	0	2 (SBA)	2	84%
Exon 5	c.668C>G	p.P223R	0	0	0	1	0	—	92%
Exon 12	c.1508A>C	p.E503A	1 (SBA)	0	0	0	0	0	—
	c.1512G>C	p.E504D	1 (SBA)	0	0	0	0	0	99%
	c.1519G>C	p.G507R	1 (An)	0	0	0	0	0	17%
	c.1525C>G	p.P509A[e]	1 (An)	0	0	0	0	0	41%
	c.1550G>C	p.S517T	0	0	0	0	1 (SBA)	0	—
	c.1570G>C	p.V524L	1 (SBA)	0	0	0	0	0	34%
Exon 14	c.1705G>A	p.A569T[f]	3 (SBA/SBO/SBO)	1	0	0	1 (SBA)	0	40%
Exon 17	c.1953T>C	p.H651H	0	1	0	0	0	—	—
Exon 19	c.2203G>T	p.V735L	0	2	0	0	0	—	81%
Intron 19	c.2316-1G>A	splice	1 (SBA)	0	0	0	0	—	
Exon 20	c.2380G>A	p.A794T	2 (SBASBA)	0	0	0	2 (SBA)	2	88%
	c.2406G>A	p.A802A	1 (An)	0	0	0	0	0	—
Exon 21	c.2474G>A	p.G825D	0	0	1 (An)	0	0	—	24%
	c.2487C>T	p.A829A	0	1	0	0	0	—	—
	c.2565A>C	p.A855A	1 (An)	0	0	0	0	—	—
Exon 23	c.2746C>T	p.L916L	1 (Crn)	0	0	0	0	—	—
Exon 25	c.2964G>A	p.R988R	0	0	0	0	1 (SBA)	0	—
	c.2965A>G	p.I989V	0	1	0	0	0	0	130%
GCSH									
Exon 1	c.53C>T	p.A18V	1 (An)	1	0	0	—	—	

All nucleotide changes were found in heterozygous form. One individual carried c.52G>T and c.1705G>A in *GLDC*, whereas no other individuals carried more than one of the nucleotide changes listed here. Eight silent polymorphisms and four missense variants present in dbSNP (http://www.ncbi.nlm.nih.gov/projects/SNP/) are not listed in this table and include: *AMT*: c.954G>A (p.R318R, rs11715915); *GLDC*: c.249G>A (p.G83G, rs12341698), c.438G>A (p.T146T, rs13289273), c.501G>A (p.E167E, rs13289273), c.660C>T (p.L220L, rs2228095), c.666T>C (p.D222D, rs12004164), c.671G>A (p.R224H, rs28617412) and c.1384C>G (p.L462V, rs73400312); and for *GCSH*: c.62T>C (p.S21L, rs8052579), c.90C>G (p.P30P, rs8177847), c.159C>T (p.F53F, rs177876), c.218A>G (N73S, rs8177876), c.252T>C (Y84Y, rs8177907) and c.261C>G (L87L, rs8177908). Grey shading indicates loss-of-function mutations, based on enzymatic activity in the *in vitro* expression study or splicing defect.

[a]Residual enzymatic activity of GLDC mutant protein is expressed as %activity of the wild-type enzyme (Fig. 2).

[b]SBA, spina bifida aperta; SBO, spina bifida occulta; An, anencephaly; Crn, craniorachischisis.

[c]Total number of UK, Japanese or Swedish NTD patients.

[d]This variant was previously established as likely to be a non-functional polymorphism by segregation in an NKH family (21).

[e]A biochemical test of folate metabolism, the dU suppression test, was previously performed on primary fibroblasts derived from this patient and showed a defect of thymidylate biosynthesis to be present (14).

[f]p.A569T has previously been reported as a pathogenic mutation in a patient with typical NKH (21).

In *AMT*, we identified two novel sequence variants predicted to result in non-synonymous missense changes, c.589G>C (D197H) and c.850G>C (V284L), in anencephaly and spina bifida patients, respectively, from the UK cohort (Table 1). Neither variant was present in 526 UK or 36 Japanese control subjects or in the SNP databases dbSNP and 1000 Genomes. An additional missense variant, E211K, was also identified in three spina bifida patients, two from the UK and one from Sweden. Causative mutations in *AMT* have been found previously in an autosomal recessive inborn error of metabolism, non-ketotic hyperglycaemia (NKH) (17). The E211K variant had previously been identified in an NKH family but was established as likely to be a non-functional polymorphism by segregation (21). Therefore, this variant is considered unlikely to be causally related to NTDs.

Exon sequencing of *GCSH* revealed eight single-base substitutions, one of which (c.53C>T, p.A18V) was a novel change found in both an NTD and a single control (Table 1). The others all corresponded to known SNPs, which did not suggest a role for *GCSH* in NTDs.

Next we turned our attention to *GLDC*, in which we identified 27 single-base substitutions (Table 1), including 11 silent nucleotide changes, 15 non-synonymous changes and a splicing acceptor variant of intron 19 (c.2316-1G>A). The

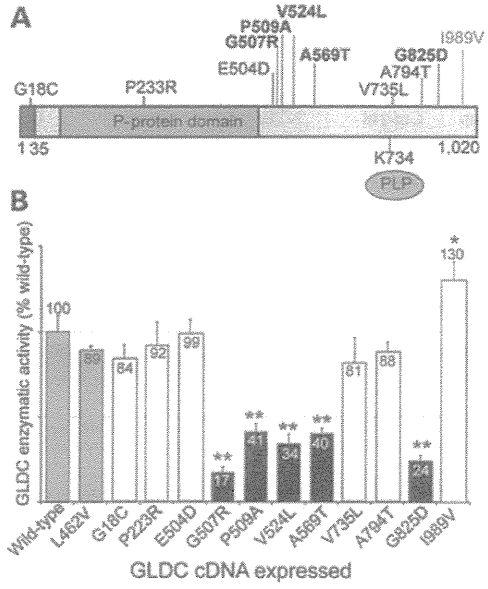

Figure 2. Characterization of *GLDC* missense mutations identified through DNA sequence analysis. (**A**) The schematic represents the 1020 amino acid residue GLDC polypeptide with the positions of the identified missense variants indicated. Mutations conferring significantly reduced activity (**B**) are indicated in bold. The leader peptide for mitochondrial import (shaded black) and the lysine 754-binding site for the co-factor pyridoxal phosphate (PLP) are indicated (49). (B) Enzymatic activity of GLDC missense variants. Expression vectors with wild-type and mutant *GLDC* cDNAs were transfected into COS7 cells for the evaluation of GLDC activity, which is expressed as relative activity (%) of cells expressing wild-type cDNA (shaded grey). The L462V GLDC enzyme (shaded grey) was tested as an example of a normally occurring variant (rs73400312). Variant proteins whose activities were significantly diminished compared with wild-type are indicated by black shading. The I989V variant, identified in a control parent, showed significantly elevated activity. Values are given as mean ± SD of triplicate experiments ($^{*}P < 0.05$; $^{**}P < 0.01$, compared with wild-type).

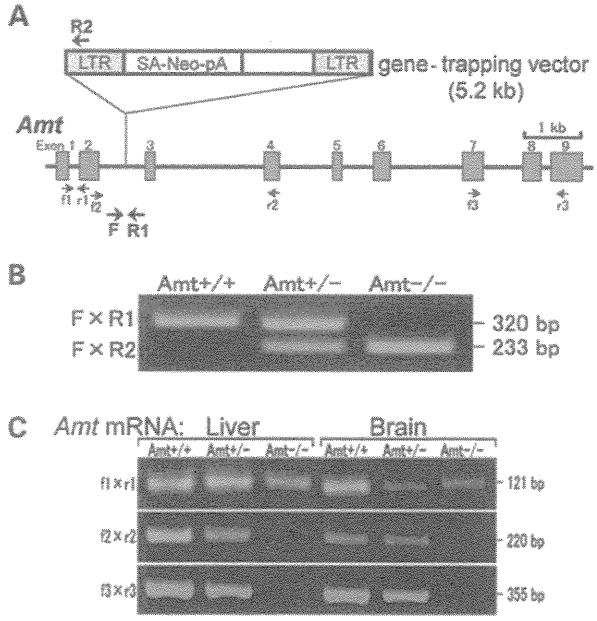

Figure 3. Generation of *Amt* knockout mouse by gene trapping. (**A**) The location of the gene-trap vector in *Amt* intron 2 in the ES cell line OST181110 was determined by inverse PCR. Mice carrying this mutation were generated using standard methods of blastocyst microinjection with OST181110 ES cells to generate chimeras, and germ-line transmission. LTR, long terminal repeats; SA, splicing acceptor site; Neo, neomycin phosphotransferase gene; pA, polyadenylation sequence. (**B**) For genotyping, mouse genomic DNA was subjected to allele-specific amplification with F, R1 and R2 primers (Supplementary Material, Table S1). A genomic fragment of 320 bp was amplified from the wild-type allele, whereas a 233 bp fragment was amplified from the *Amt*-mutant allele. (**C**) RT-PCR analysis of *Amt* mRNA expressed in the brain and liver of *Amt*-mutant mice. Primers in exon 1–2 generated a 121 bp band irrespective of mouse genotypes. RT-PCR in which either one (f2-r2) or both (f3-r3) primers were located in exons 3′ to the insertion site produced 220 and 355 bp cDNA fragments, respectively, in $Amt^{+/+}$ and $Amt^{+/-}$ mice, but not in $Amt^{-/-}$. The *Amt* mRNA in mice carrying the trap vector was, therefore, aberrantly spliced at the end of exon 2, resulting in truncation of *Amt* mRNA in $Amt^{-/-}$ mice.

latter is deduced to abolish normal splicing of the *GLDC* mRNA, with predicted skipping of exon 19 resulting in loss of the reading frame. Among the 15 missense variants identified in *GLDC*, 5 were unique to the NTD group, being absent from all 562 control individuals as well as from the SNP databases. A further three novel variants were found only in controls, whereas the remainder were found in both NTDs and controls, and included previously reported SNPs.

We investigated the possible functional effects of *GLDC* missense variants by expressing wild-type and mutant cDNA constructs in COS7 cells, followed by enzymatic assay of GLDC activity involving a decarboxylation reaction using [1-^{14}C]glycine (22). Twelve GLDC variants were tested, including those that were unique to NTD patients and, therefore, hypothesized to be potentially pathogenic (Fig. 2). The L462V variant, which corresponds to a known SNP (rs73400312), was included as an example of a known normally occurring form. Five of the missense changes, G507R, P509A, V524L, A569T and G825D, resulted in a significant reduction in GLDC activity compared with the wild-type protein ($P < 0.001$). Notably, all five of these deleterious variants were present solely in NTD cases, whereas none of the variants that were unique to controls (P223R, V735L and I989V) showed loss of enzymatic function. In the case of G18C and A794T, which occurred in both NTDs and controls, there was no significant loss of enzymatic activity, suggesting that these are unlikely to be causative mutations.

Having identified putative mutations in *AMT* and *GLDC* in NTD patients, we hypothesized that loss of GCS function could predispose to development of NTDs. In order to directly test the functional requirement for GCS activity in neural tube closure, we generated mice that lacked GCS activity, using a gene trap (OmniBank, OST181110) of the *Amt* gene. The vector was located in intron 2, resulting in a truncated transcript that lacked exons 3–9 (Fig. 3). The efficacy of the gene-trap vector in trapping expression of *Amt* (Amt^{-}) was confirmed by RT-PCR analysis (Fig. 3). Heterozygous $Amt^{+/-}$ mice were viable and fertile and exhibited no obvious malformations. Homozygous $Amt^{-/-}$ mice were not observed among post-natal litters from heterozygote intercrosses, and so fetuses were examined at embryonic day (E) 17.5. Strikingly, 87% of $Amt^{-/-}$ fetuses (34 out of 39) exhibited NTDs, whereas no malformations were observed in $Amt^{+/+}$ ($n = 33$) or $Amt^{+/-}$

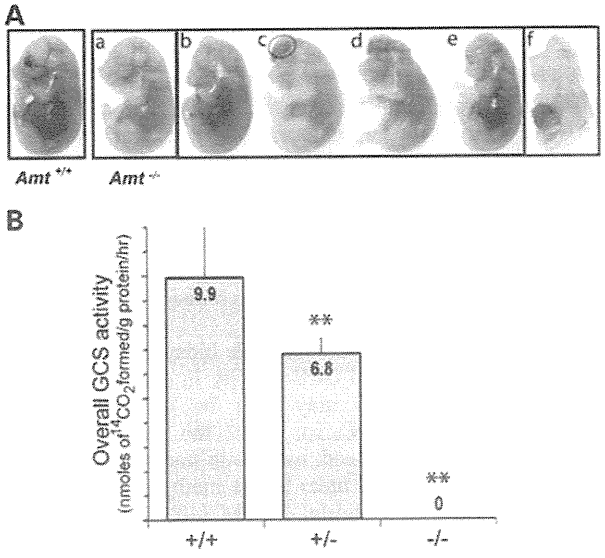

Figure 4. Mice lacking GCS activity exhibit NTDs. (**A**) Phenotypes of *Amt* mutant mice. NTDs were evident in the majority (88%) of $Amt^{-/-}$ fetuses (examples shown are at E17.5). Various types of NTDs were observed in $Amt^{-/-}$ fetuses, which principally affected the cranial region; a, no NTDs; b, small exencephaly (dotted circle); c–e, large exencephaly; f, craniorachischisis. (**B**) Enzymatic activity of the GCS in *Amt* knockout mice. $Amt^{+/-}$ and $Amt^{-/-}$ fetuses had significantly lower GCS activity in the liver than $Amt^{+/+}$ fetuses, with activity in $Amt^{-/-}$ samples below the level of detection (**$P < 0.01$ compared with $Amt^{+/+}$).

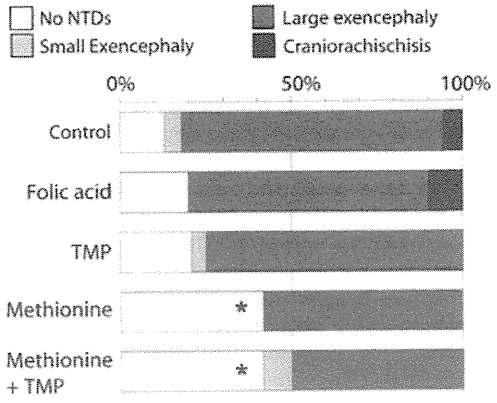

Figure 5. Maternal supplementation of *Amt* mutant embryos with folic acid, TMP or methionine. Maternal treatment with folic acid ($n = 10$ homozygous mutant fetuses) or TMP ($n = 12$) had no significant effect on NTD frequency, whereas the frequency of unaffected embryos was significantly increased following treatment with methionine ($n = 12$) or methionine plus TMP group ($n = 12$). The asterisk indicates significant difference compared with non-treated group ($P < 0.05$).

($n = 66$) fetuses. Defects mainly comprised exencephaly (82%), in which the cranial neural folds persistently failed to close (Fig. 4). There was also a low frequency of the more severe condition, craniorachischisis (5%), in which the neural tube remains open from the mid- and hindbrain, and throughout the spinal region (Fig. 4). Fetal liver samples were subjected to enzyme assay to determine overall activity of the GCS. In $Amt^{-/-}$ mice, overall GCS activity was effectively ablated being below the detection level of the assay (0.01 nmoles of $^{14}CO_2$ formed/gram protein/h), consistent with the Amt^{-} allele being a functional null (22) (Fig. 4). These findings confirm that AMT function is essential for GCS activity, and that the latter is necessary for successful neural tube closure.

Given that GCS is a component of FOCM (Fig. 1), we evaluated the possible prevention of NTDs by folate-related metabolites. Maternal supplementation was performed with folic acid, thymidine monophosphate (TMP), methionine or methionine plus TMP (23). Neither folic acid nor TMP significantly affected the frequency of NTDs among the homozygous $Amt^{-/-}$ offspring. However, we observed a significant protective effect of maternal supplementation with methionine or methionine plus TMP, compared with the non-treated group ($P < 0.05$; Fig. 5).

DISCUSSION

NTDs remain among the commonest human birth defects and understanding their genetic basis presents a considerable challenge owing to their multigenic inheritance and the potential influence of environmental factors, either predisposing or ameliorating. Several lines of evidence indicate a requirement for FOCM in neural tube closure and, therefore, GCS-encoding genes provide excellent candidates for possible involvement in NTD susceptibility. We identified putative mutations in *AMT* and *GLDC* which include a splice acceptor mutation and a number of non-synonymous variants that were absent from a large group of population-matched controls, as well as from public SNP databases. In the case of *GLDC*, enzymatic assay confirmed that several mutations resulted in significant loss of enzyme activity. Finally, *in vivo* functional evidence of a requirement for GCS function in neural tube closure was provided by the occurrence of NTDs in $Amt^{-/-}$ mice lacking GCS activity. Together these findings indicate that mutations in *GLDC* and *AMT* predispose to NTDs in both mice and humans.

Where parental samples were available (6 of the 11 NTD cases that involved putative mutations in *GLDC*), we demonstrated parent-to-child transmission (Supplementary Material, Table S2). Six were instances of maternal transmission and one involved paternal transmission. We hypothesize that absence of an overt NTD phenotype in parents who carry a deficient *GLDC* allele may result from incomplete penetrance, or lack of additional genetic or environmental factors which are predicted to be necessary for NTDs owing to their multifactorial aetiology. We also note that partial penetrance is a feature of numerous mouse models of NTDs (5,8).

Inherited GCS deficiency, owing to mutation of *AMT* and/or *GLDC*, has been shown to cause NKH in humans (17). NKH is a rare, autosomal recessive, inborn error of metabolism, characterized by accumulation of glycine and encephalopathy-like neurological signs, including coma and convulsive seizures in neonates. GCS activity is greatly diminished in NKH patients and they would, therefore, be predicted to be at increased risk of NTDs. It is possible that NTDs may occur in combination with NKH but as anencephaly is a lethal condition, co-existing